
Test-Time Adaptation via Self-Training with Nearest Neighbor Information

Minguk Jang, Sae-Young Chung

School of Electrical Engineering, KAIST, Republic of Korea
{mgjang, schung}@kaist.ac.kr

Abstract

Adapting trained classifiers using only online test data is important since it is difficult to access training data or future test data during test time. One of the popular approaches for test-time adaptation is self-training, which fine-tunes the trained classifiers using the classifier predictions of the test data as pseudo labels. However, under the test-time domain shift, self-training methods have a limitation that learning with inaccurate pseudo labels greatly degrades the performance of the adapted classifiers. To overcome this limitation, we propose a novel test-time adaptation method *Test-time Adaptation via Self-Training with nearest neighbor information (TAST)*. Based on the idea that a test data and its nearest neighbors in the embedding space of the trained classifier are more likely to have the same label, we adapt the trained classifier with the following two steps: (1) generate the pseudo label for the test data using its nearest neighbors from a set composed of previous test data, and (2) fine-tune the trained classifier with the pseudo label. Our experiments on two standard benchmarks, i.e., domain generalization and image corruption benchmarks, show that TAST outperforms the current state-of-the-art test-time adaptation methods.

1 Introduction

Poor generalization ability has been pointed out as a critical problem in deep learning. The performance degradation caused by domain shift (i.e., distribution shift) between training and test domains can be found in various tasks such as classification [49, 54], visual recognition [7, 42], and reinforcement learning [6, 29, 36]. There are two broad classes of domain adaptation methods that attempt to solve this problem: supervised domain adaptation (SDA) [38, 50] and unsupervised domain adaptation (UDA) [14, 35, 43]. SDA and UDA methods aim to obtain domain-invariant representations by aligning the representations of training and test data closely in the embedding space. While testing, UDA methods require the training dataset and SDA methods additionally require labeled data of the test domain. However, it is practically difficult to access training datasets or labeled data of the test domain during test time due to data security or labeling cost.

Test-time adaptation (TTA) [22, 53] is a prominent approach to alleviate the problem caused by domain shift. TTA methods aim to adapt the trained model to the test domain without a labeled dataset in the test domain and any information related to the training procedure (e.g., training dataset, feature statistics/momentum of training domain [9, 34, 47]). TTA methods have access to the online unlabeled test data only, whereas domain adaptation methods have access to the whole (i.e., offline) test data.

One popular category of TTA methods is based on entropy minimization [32, 53]. Entropy minimization methods aim to obtain feature representations that are well classified by the trained classifier. Thus such methods fine-tune the trained feature extractor, which is the rest of the trained classifier except the last linear layer, by minimizing the prediction entropy of test data. These methods force the

classifier to have over-confident predictions for test data. It has a risk of degrading model calibration [16, 39], used as a measure of model interpretability and reliability. One form of entropy minimization is self-training [1, 28, 40, 58]. Self-training methods use classifier predictions as pseudo labels for the test data and fine-tune the classifier to predict the label of the unlabeled data as the pseudo label. These methods have a limitation in that the fine-tuned classifier can overfit to the inaccurate pseudo labels (i.e., confirmation bias [1]). This limitation can be harmful when the performance of the trained classifier is significantly degraded due to domain shift. To avoid this limitation, Lee [28] proposed a self-training method that fine-tunes the classifier using only the test data with a confident pseudo label, but the confidence threshold for selecting the confident pseudo labels needs to be determined manually.

On the other hand, Iwasawa and Matsuo [22] recently proposed a prototype-based TTA method named T3A. T3A first constructs pseudo-prototypes that represent classes in the embedding space using a support set composed of previous test data and their predictions. Then, T3A uses nearest neighbor information to predict the label of the test data. Specifically, T3A predicts the label of the test data as the class of the nearest pseudo-prototype. T3A does not modify network parameters during test time (i.e., optimization-free), whereas network training methods considering the nearest neighbor information have shown strong performance in the fields of metric learning [24, 60], representation learning [3, 4, 8, 23], semi-supervised learning [20, 55], and few-shot learning [44, 52, 56].

Our contributions are summarized as follows:

- In this paper, we propose a novel method *Test-time Adaptation via Self-Training with nearest neighbor information (TAST)* that alleviates the limitation of self-training due to inaccurate pseudo labels by utilizing the nearest neighbor information in the embedding space. Based on the idea that a test data and its nearest neighbors in the embedding space are more likely to have the same label, TAST assigns the mean of the labels of the nearby support examples as the pseudo label for the test data. Then the trained classifier is fine-tuned to predict the label of the unlabeled test data as the pseudo label. (Section 3)
- We develop an ensemble scheme for test-time adaptation. Ensemble schemes [37, 57, 63] refer to methods of combining independently trained classifiers to obtain more robust and accurate predictions than those of a single classifier. When a single trained classifier is given at test time, we construct an ensemble scheme by attaching multiple projection heads after the frozen feature extractor. The projection heads are randomly initialized at the beginning of the test time, and they are trained by using the pseudo labels as a supervisory signal. We predict the label of test data using the average predicted class distribution from the projection heads.
- We investigate the effectiveness of TAST on two standard benchmarks, i.e., domain generalization and image corruption benchmarks, to evaluate generalization to domain shift and common image corruptions, respectively. We observe that TAST consistently improves the performance of the trained classifier and outperforms existing test-time adaptation methods including the state-of-the-art on most of the benchmarks. Particularly, TAST surpasses the current state-of-the-art algorithm by 1.01% and 0.69% on average with ResNet-18 and ResNet-50 networks learned by Empirical Risk Minimization (ERM) on the domain generalization benchmarks, respectively. *TAST-BN*, which is a variant of TAST having different fine-tuning layers, outperforms the state-of-the-art method by 1.24% on average on the image corruption benchmark. Extensive ablation studies show that the nearest neighbor information and the ensemble scheme contribute to the performance increase. (Section 4)

2 Preliminaries

Test-time domain shift Consider a labeled dataset $D^{\text{train}} = \{(x_i, y_i)\}_{i=1}^{n_{\text{train}}}$ drawn from a distribution P^{train} , where $x \in \mathbb{R}^d$ and $y \in \mathcal{Y} := \{1, 2, \dots, K\}$ for a K -class classification problem. A number of classifiers have been proposed that easily classify unseen test data under the i.i.d. assumption that unseen test data D^{test} is drawn from the same distribution as training data, i.e., $P^{\text{train}} = P^{\text{test}}$. We assume the classifier is a deep neural network composed of two parts: a feature extractor $f_\theta : \mathbb{R}^d \rightarrow \mathbb{R}^{d_z}$ and a linear classifier $g_w : \mathbb{R}^{d_z} \rightarrow \mathcal{Y}$, where θ and w are the neural network parameters. ERM optimizes θ and w to obtain a good classifier for future samples in D^{test} by minimizing the objective function $\mathcal{L}(\theta, w) = \mathbb{E}_{(x,y) \in D^{\text{train}}} [l(g_w(f_\theta(x)), y)]$, where l is a loss function

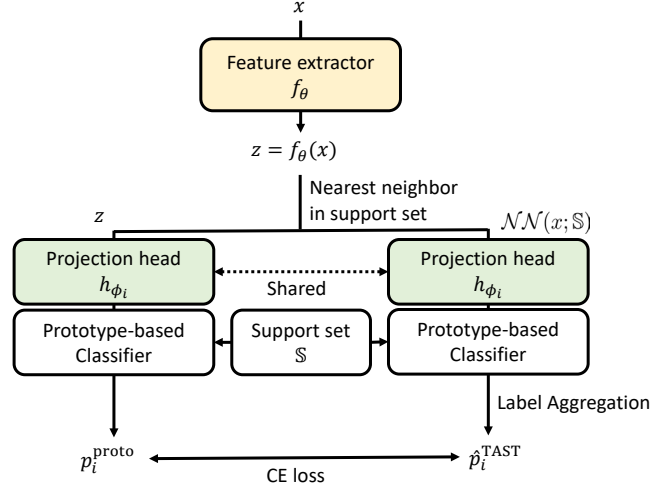


Figure 1: Overview of TAST training for each projection head. Based on the intuition that a test data x and its nearest neighbors $\mathcal{NN}(x; \mathbb{S})$ are likely to share the same label, we use the mean of prototype-based predictions of the support examples in $\mathcal{NN}(x; \mathbb{S})$ as the pseudo label of x . We train the projection heads to predict the pseudo labels when the test data is fed into. Notice that the feature extractor is frozen during test time.

such as cross-entropy loss. However, under the test-time domain shift (i.e., distribution shift), the i.i.d. assumption between the training and test distributions does not hold, i.e., $P^{\text{train}} \neq P^{\text{test}}$, and the trained classifiers often show poor classification performance for the test data.

Test-time adaptation Test-time adaptation (TTA) methods adapt a trained classifier without any information related to the training procedure such as training dataset during test time. Self-training uses classifier predictions as pseudo labels for unlabeled test data and fine-tunes the classifier with the pseudo labels. To avoid the confirmation bias induced by wrong pseudo labels, the trained classifier is fine-tuned using only the data having confident pseudo labels above a threshold. Formally, let $p(y|x)$ be the likelihood the classifier assigns x to the class y . The pseudo label of x is obtained as $\hat{p} = \arg \max_c p(c|x)$. Self-training methods use the following loss function for fine-tuning:

$$\mathcal{L}(\theta, w) = \frac{1}{|D^{\text{test}}|} \sum_{x \in D^{\text{test}}} \mathbb{1}[\max_c p(c|x) \geq \tau] \text{CE}(\hat{p}, p(Y|x)), \quad (1)$$

where τ represents the confidence threshold and CE denotes the standard cross-entropy loss.

Prototype-based classification refers to a method that obtains prototype representations, which represent classes in the embedding space, and then predicts the label of an input as the class of the nearest prototype. Since labeled data is not available in the TTA setting, T3A [22] utilizes a support set that is composed of previous test data and their predictions by the trained classifier. Moreover, T3A does not modify parameters of the classifier. Since the embedding space of the feature extractor is unchanged during the test time, T3A constructs the support set using the feature representations for test data instead of the data itself. Specifically, a support set $\mathbb{S}_t = \{\mathbb{S}_t^1, \mathbb{S}_t^2, \dots, \mathbb{S}_t^K\}$ is a set of test samples until time t . The support set is initialized with the weight of the last linear classifier, i.e., $\mathbb{S}_0^k = \left\{ \frac{w^k}{\|w^k\|} \right\}$, where w^k is the parts of w related to k -th class for $k = 1, 2, \dots, K$. At time t , the support set is updated as

$$\mathbb{S}_t^k = \begin{cases} \mathbb{S}_{t-1}^k \cup \left\{ \frac{f_\theta(x_t)}{\|f_\theta(x_t)\|} \right\} & \text{if } \arg \max_c p_c = k \\ \mathbb{S}_{t-1}^k & \text{otherwise,} \end{cases} \quad (2)$$

where p_k represents the likelihood the classifier assigns x_t to the k -th class. Using the support set \mathbb{S}_t^k , one can obtain the class prototype for class k by taking the centroid of the representations in the support set. Formally, the prototype μ_k for class k is computed as $\mu_k = \frac{1}{|\mathbb{S}_t^k|} \sum_{z \in \mathbb{S}_t^k} z$ for $k = 1, 2, \dots, K$. Then, the prediction for an input x_t is made by comparing the distances between

Algorithm 1 TAST

Require: Feature extractor f_θ , projection heads $\{h_{\phi_i}\}_{i=1}^{N_e}$, test batch \mathbb{B} , support set \mathbb{S} , number of iterations per adaptation T , number of support examples per each class M , number of nearby support examples N_s , learning rate α

Ensure: Predictions for all $x \in \mathbb{B}$

Update the support set \mathbb{S} with eq. (2) and (3)

Retrieve the nearest neighbors $\mathcal{NN}(x; \mathbb{S})$ for all $x \in \mathbb{B}$ with eq. (4)

for $t = 1 : T$ **do**

for $i = 1 : N_e$ **do**

for $x \in \mathbb{B}$ **do**

 Obtain the nearest neighbor-based pseudo label $\hat{p}_i^{\text{TAST}}(Y|x)$ of x with eq. (7)

 Compute the prototype-based class distribution $p_i^{\text{proto}}(Y|x)$ of x with eq. (9)

end for

$\phi_i \leftarrow \phi_i - \alpha \nabla_{\phi_i} \frac{1}{|\mathbb{B}|} \sum_{x \in \mathbb{B}} \text{CE}(\hat{p}_i^{\text{TAST}}(Y|x), p_i^{\text{proto}}(Y|x))$

end for

end for

Compute the predictions for all $x \in \mathbb{B}$ with eq. (10)

the embedding of x_t and the prototypes, i.e., $\hat{y} = \arg \min_c d(f_\theta(x_t), \mu_c)$ with a pre-defined metric d such as Euclidean distance or cosine similarity.¹ Such support set construction can cause two major problems: (1) the size of the support set steadily increases, and (2) the wrongly pseudo labeled examples could be included in the support set, which can degrade the classification performance. To alleviate these problems, the support examples with unconfident pseudo labels are regarded as unreliable examples and they are filtered out, i.e., at time stamp t ,

$$\mathbb{S}_t^k = \{z | z \in \mathbb{S}_t^k, H(\sigma(g_w(z))) \leq \alpha_k\}, \quad (3)$$

where α_k is the M -th largest prediction entropy of the samples from \mathbb{S}_t^k , H is Shannon entropy [33], and σ is the softmax function.

3 Methodology

We consider the layers to be fine-tuned in the trained classifier before explaining our test-time adaptation method. One possible choice is to fine-tune the whole network parameters in the classifier during test time, but it can be unstable and inefficient [27, 53]. Another choice is to fine-tune only the parameters of batch normalization (BN) layers in the classifier as in [53]. Although it achieves effective test-time adaptation, it has a limitation that it can be utilized only if there are BN layers in the trained classifier. The other choice is to train a new classifier attached after the frozen feature extractor during test time. We construct the new classifier by attaching a randomly initialized projection head as illustrated in Figure 1. During the test time, we train the projection head and predict the label of the test data using prototype-based class distributions in the embedding space of the projection head. Furthermore, we can consider an ensemble scheme that uses multiple projection heads. We train the projection heads independently and predict the label of the test data using the average predicted class distribution from the projection heads.

In this section, we describe our method named TAST that uses multiple projection heads. TAST is mainly composed of (1) generating pseudo labels for unlabeled test data with the nearest neighbor information and (2) fine-tuning the trained classifier with the pseudo labels. The whole adaptation procedure of TAST is described in Algorithm 1. We first update the support set \mathbb{S} and filter out the unconfident examples from the support set as in [22] with the equations (2) and (3). Then, we find N_s nearby support examples of test data x in the embedding space of f_θ . We denote $\mathcal{NN}(x; \mathbb{S})$ as the set of nearby support examples of x ,

$$\mathcal{NN}(x; \mathbb{S}) := \{z \in \mathbb{S} | d(f_\theta(x), z) \leq \beta_x\}, \quad (4)$$

where β_x is the distance between x and the N_s -th nearest neighbor of x from \mathbb{S} in the embedding space of f_θ . Each projection head is trained individually during test time. For the i -th projection head, we compute the prototype representations $\mu_{i,1}, \mu_{i,2}, \dots, \mu_{i,K}$ in the embedding space of $h_{\phi_i} \circ f_\theta$

¹We use the cosine similarity for experiments throughout this paper.

with a support set $\mathbb{S} = \{\mathbb{S}^1, \mathbb{S}^2, \dots, \mathbb{S}^K\}$, i.e., $\mu_{i,k} = \frac{1}{|\mathbb{S}^k|} \sum_{z \in \mathbb{S}^k} h_{\phi_i}(z)$, for $k = 1, 2, \dots, K$. With the prototypes, we compute the prototype-based predicted class distribution of the nearby support examples in the embedding space of $h_{\phi_i} \circ f_{\theta}$, i.e., for $z \in \mathcal{N}\mathcal{N}(x; \mathbb{S})$, the likelihood that the prototype-based classifier assigns z to the k -th class is computed as

$$p_i^{\text{proto}}(Y = k|z) := \frac{\exp(-d(h_{\phi_i}(z), \mu_{i,k})/\tau)}{\sum_c \exp(-d(h_{\phi_i}(z), \mu_{i,c})/\tau)}, \quad (5)$$

where τ is the softmax temperature.² With the nearest neighbor information, TAST generates an estimated class distribution p_i^{TAST} and a pseudo label \hat{p}_i^{TAST} of x by aggregating prototype-based predicted class distribution of the nearby support examples in $\mathcal{N}\mathcal{N}(x; \mathbb{S})$ as

$$p_i^{\text{TAST}}(Y = k|x) := \frac{1}{N_s} \sum_{z \in \mathcal{N}\mathcal{N}(x; \mathbb{S})} p_i^{\text{proto}}(Y = k|z) \quad (6)$$

$$\hat{p}_i^{\text{TAST}}(Y = k|x) := \frac{1}{N_s} \sum_{z \in \mathcal{N}\mathcal{N}(x; \mathbb{S})} \mathbb{1}[\arg \max_c p_i^{\text{proto}}(Y = c|z) = k], \quad (7)$$

for $k = 1, 2, \dots, K$. Especially, we use the one-hot class distributions for pseudo label generation as in [28, 45]. Then, we fine-tune the classifier by minimizing the cross-entropy loss between the predicted class distribution of the test example and the pseudo label using the nearby support examples:

$$\mathcal{L}^{\text{TAST}}(\phi_i) = \frac{1}{|D^{\text{test}}|} \sum_{x \in D^{\text{test}}} \text{CE}(\hat{p}_i^{\text{TAST}}(Y|x), p_i^{\text{proto}}(Y|x)), \quad (8)$$

$$p_i^{\text{proto}}(Y = k|x) := \frac{\exp(-d(h_{\phi_i}(f_{\theta}(x)), \mu_{i,k})/\tau)}{\sum_c \exp(-d(h_{\phi_i}(f_{\theta}(x)), \mu_{i,c})/\tau)}, \quad k = 1, 2, \dots, K. \quad (9)$$

We iterate the pseudo labeling and fine-tuning processes for T steps per batch. Finally, we predict the label of x using the average predicted class distribution from the projection heads, i.e.,

$$\hat{y}^{\text{TAST}} = \arg \max_c p^{\text{TAST}}(c|x) = \arg \max_c \frac{1}{N_e} \sum_{i=1}^{N_e} p_i^{\text{TAST}}(c|x). \quad (10)$$

On the other hand, for the case when BN layers exist in the feature extractor, we consider a variant of TAST, named TAST-BN, that fine-tunes the BN layers instead of projection heads. The support set stores the test data itself instead of the feature representations since the embedding space of the feature extractor steadily changes during the test time. The pseudocode for TAST-BN is presented in Appendix B.

4 Experiments

In this section, we show the effectiveness of our method compared to the state-of-the-art test-time adaptation methods on two standard benchmarks, i.e., domain generalization and image corruption benchmarks.

We compare TAST with the following baseline methods: (1) Pseudo Labeling (PL) [28] fine-tunes the trained classifier using confident pseudo labels based on classifier predictions; (2) PLCIf is a modified version of PL that fine-tunes only the last linear classifier; (3) Tent [53] fine-tunes only the parameters of the BN layers to minimize the prediction entropy of test data; (4) TentBN is a modified version of Tent that adds a BN layer between the feature extractor and the last linear classifier, and fine-tunes only the added BN layer; (5) TentClf is a modified version of Tent that fine-tunes only the last linear classifier instead of the BN layers; (6) SHOTIM [32] updates the feature extractor to maximize the mutual information between an input and its prediction; (7) SHOT is a method that adds a pseudo-label loss to SHOTIM; (8) T3A predicts the label of the test data by comparing distances between test data and the generated pseudo-prototypes. Originally, SHOT is one of source-free domain adaptation methods which focus on the offline setting, but we compare our method with the online version of SHOT for a fair comparison.

²We set $\tau = 0.1$ for experiments throughout this paper.

Table 1: Average accuracy (%) using classifiers learned by ERM on the domain generalization benchmarks. We use ResNet-18 and ResNet-50 as backbone networks. **Bold** indicates the best performance for each benchmark. Our proposed method TAST outperforms all the baselines on all of the benchmarks.

Method	Backbone	VLCS	PACS	OfficeHome	TerraIncognita	Avg	
ERM	ResNet-18	74.88±0.46	79.29±0.77	62.10±0.31	40.62±1.19	64.22	
+Tent		72.88±0.82	83.89±0.54	60.86±0.39	33.70±1.09	62.83	
+TentBN		67.02±1.16	80.75±1.01	62.64±0.38	39.91±0.76	62.58	
+TentClf		72.96±1.48	78.57±1.78	59.33±0.62	38.30±3.44	62.29	
+SHOT		65.24±2.29	82.36±0.63	62.58±0.39	33.57±1.04	60.94	
+SHOTIM		64.86±2.22	82.33±0.61	62.57±0.39	33.35±1.23	60.78	
+PL		62.97±2.72	70.98±1.78	58.20±3.21	37.44±7.20	57.40	
+PLClf		74.89±0.61	78.11±2.30	61.92±0.41	41.78±1.94	64.18	
+T3A		77.26±1.49	80.83±0.67	63.21±0.50	40.20±0.60	65.38	
+TAST (Ours)		77.27±0.67	81.94±0.44	63.70±0.52	42.64±0.72	66.39	
+TAST-BN (Ours)		75.21±2.36	87.07±0.53	62.79±0.41	39.43±2.24	66.13	
ERM		ResNet-50	76.71±0.50	83.21±1.14	67.13±0.99	45.93±1.34	68.25
+Tent			72.96±1.27	85.16±0.62	66.29±0.77	37.08±2.04	65.37
+TentBN	69.65±1.17		83.69±1.16	67.91±0.89	43.89±1.25	66.29	
+TentClf	75.80±0.68		82.66±1.59	66.79±0.98	43.64±2.59	67.22	
+SHOT	67.07±0.90		84.07±1.23	67.65±0.72	35.20±0.82	63.50	
+SHOTIM	66.93±0.84		84.14±1.25	67.65±0.77	34.37±1.07	63.27	
+PL	69.41±3.12		81.72±4.61	62.85±3.05	38.09±2.35	63.02	
+PLClf	75.65±0.88		83.33±1.59	67.01±1.00	46.66±2.12	68.16	
+T3A	77.29±0.39		83.92±1.13	68.26±0.84	45.61±1.10	68.77	
+TAST (Ours)	77.66±0.48		84.11±1.22	68.63±0.70	47.43±2.09	69.46	
+TAST-BN (Ours)	73.52±1.37		89.16±0.47	68.88±0.50	41.47±2.88	68.26	

4.1 Domain Generalization

The domain generalization benchmarks are designed to evaluate the generalization ability of the trained classifiers to the unseen domain. The evaluation is performed by a leave-one-domain-out procedure, which uses a domain as a test domain and the remaining domains as training domains. We use the publicly released code <https://github.com/matsuo1ab/T3A> for the domain generalization benchmarks.

4.1.1 Experimental setup

Datasets We test TAST on four domain generalization benchmarks, specifically VLCS [11], PACS [30], OfficeHome [51], and TerraIncognita [2]. VLCS is composed of photographic images from four different datasets (PASCAL VOC207 [10], LableMe [41], Caltech 101 [12], and SUN09 [5]), consisting of 10,729 examples of 5 categories (bird, car, chair, dog, and person). PACS is composed of images of objects from four different domains (photo, art, cartoon, and sketch), consisting of 9,991 examples of 7 categories (dog, elephant, giraffe, guitar, horse, house, and person). OfficeHome is composed of images of objects in the office and home from 4 different domains (artistic images, clip art, product, and real-world images), consisting of 15,588 examples of 65 categories (e.g., alarm clock, backpack, and batteries). TerraIncognita is composed of wild animal images taken from 4 different locations (L100, L38, L43, and L46), consisting of 24,788 examples of 10 classes.

Training setup For a fair comparison, we follow the training setup including dataset splits and hyperparameter selection method used in [22]. We use residual networks [18] including batch normalization layers with 18 and 50 layers (hereinafter referred to as ResNet-18 and ResNet-50, respectively), which are widely used for classification tasks. We train the networks with various learning algorithms such as ERM and CORAL [46]. Details about the learning algorithms are explained in Appendix A. The backbone networks are trained with the default hyperparameters introduced in [15]. We use a BatchEnsemble [57], which is an efficient ensemble method that reduces the computational cost by weight-sharing, for the projection heads of TAST. The output dimension of

Table 2: Average accuracy (%) on domain generalization benchmarks using classifiers trained by different learning algorithms, namely CORAL, MMD, and Mixup. We use ResNet-18 as a backbone network. **Bold** indicates the best performance for each benchmark. TAST and TAST-BN consistently improve the performance of the trained classifiers and they outperform T3A on most of the benchmarks.

Method	VLCS	PACS	OfficeHome	TerraIncognita	Avg
CORAL	74.00±1.13	81.00±0.79	62.78±0.06	36.51±2.35	63.57
+T3A	75.49±1.67	82.75±0.51	63.72±0.32	38.39±1.39	65.09
+TAST (Ours)	74.82±2.43	83.16±0.81	64.00±0.25	39.21±1.75	65.30
+TAST-BN (Ours)	77.01±0.36	87.21±0.57	62.98±0.23	37.45±1.11	66.16
MMD	74.90±0.50	81.06±0.92	62.20±0.48	35.73±2.70	63.47
+T3A	77.28±0.45	82.52±0.53	63.34±0.55	37.40±1.86	65.14
+TAST (Ours)	76.21±0.79	83.29±0.26	63.49±0.49	38.12±2.47	65.28
+TAST-BN (Ours)	76.06±0.89	86.35±0.76	63.22±0.26	39.46±1.63	66.27
Mixup	74.97±0.86	78.29±0.88	61.83±0.88	41.04±1.01	64.03
+T3A	78.43±0.76	81.91±0.54	63.49±0.86	39.89±0.90	65.93
+TAST (Ours)	77.19±0.80	82.85±0.36	63.83±0.74	41.44±1.67	66.33
+TAST-BN (Ours)	76.89±0.86	87.14±0.56	62.09±0.86	42.70±1.90	67.21

each projection head is set to a quarter of the output dimension of the feature extractor, e.g., 128 for ResNet-18. We use Kaiming normalization [17] for initializing the projection heads at the beginning of test time. We run experiments using four different random seeds. More details on the training setups can be found in Appendix A.

Hyperparameters For a fair comparison, the baseline methods use the same hyperparameters as in [22]. TAST uses the same set of possible values for each hyperparameter with baseline methods. TAST involves four hyperparameters: the number of iterations per adaptation T , the number of support examples per each class M , and the number of nearby support examples N_s , the number of projection head N_e . We define a finite set of possible values for each hyperparameter, $N_s \in \{1, 2, 4, 8\}$, $T \in \{1, 3\}$, and $M \in \{1, 5, 20, 50, 100, -1\}$, where -1 means to storing all samples without filtering. N_e is set to 20. We use Adam optimizer with a learning rate of 0.001. For TAST-BN, we restrict the size of the whole support set to 150 due to effective memory usage since the test data and the support examples are fed into together. More details on the hyperparameters can be found in Appendix A.

4.1.2 Experimental results

In Table 1, we summarize the experimental results of test-time adaptation methods using classifiers trained by ERM. Our method consistently improves the performance of the trained classifiers by 2.17% and 1.21% for ResNet-18 and ResNet-50 on average, respectively. TAST also outperforms the baseline methods including the state-of-the-art test-time adaptation method T3A. Compared to T3A, TAST shows better performance by 1.01% and 0.69% for ResNet-18 and ResNet-50 on average, respectively. Especially, we find that our method significantly improves the performance of the trained classifiers in the TerraIncognita benchmark, which is a challenging benchmark in that the trained classifier shows the lowest prediction accuracy.

In Table 2, we show the results of test-time adaptation methods using classifiers trained by three different learning algorithms, namely CORAL [46], MMD [31], and Mixup [59]. TAST consistently enhances the performance of the trained classifiers on the benchmarks by 1.73%, 1.81%, and 2.30% on average using the classifiers trained by CORAL, MMD, and Mixup, respectively. We find that TAST has a minor performance gain compared to the results in Table 1, whereas it surpasses T3A on most of benchmarks. Compared to T3A, TAST shows better performance on the benchmarks by 0.21%, 0.14%, and 0.40% on average with the classifiers trained by CORAL, MMD, and Mixup, respectively. Refer to Appendix D for the experimental results of the other baseline methods.

In Table 1, we observe that the performance of the baseline methods, which fine-tune the feature extractors, is lower than that of the classifiers without adaptation, whereas TAST-BN improves the

Table 3: Ablation studies to evaluate the effects of the number of projection head and the nearest neighbor information. We use ResNet-18 trained by ERM. TAST-N is a method that removes projection heads from TAST.

Method	N_e	VLCS	PACS	OfficeHome	TerraIncognita	Avg
ERM	-	74.88±0.46	79.29±0.77	62.10±0.31	40.62±1.19	64.22
+T3A	-	77.26±1.49	80.83±0.67	63.21±0.50	40.20±0.60	65.38
+TAST-N (Ours)	-	76.20±1.87	81.62±0.52	63.54±0.63	41.88±1.21	65.81
+TAST (Ours)	1	75.20±0.77	81.23±0.70	62.09±0.64	42.59±0.41	65.28
	5	76.68±0.77	81.81±0.13	63.51±0.59	42.68±0.80	66.17
	10	77.43±0.62	81.56±0.85	63.39±0.56	42.60±0.63	66.25
	20	77.27±0.67	81.94±0.44	63.70±0.52	42.64±0.72	66.39

performance of the trained classifiers. As shown in Table 2, TAST-BN shows better performance than TAST on the benchmarks by 0.86%, 0.99%, and 0.88% on average with the classifiers trained by CORAL, MMD, and Mixup, respectively.

Effect of nearest neighbor information To understand the effect of nearest neighbor information, we compare Tent and TAST-BN. To fine-tune the BN layers, Tent uses entropy minimization loss, whereas TAST-BN uses the pseudo-label loss using the nearby support examples. In Table 1, the performances of TAST-BN is better than those of Tent by 3.3% and 2.89% for ResNet-18 and ResNet-50, respectively.

In addition, we consider an ablated variant of TAST, named TAST-N, that removes projection heads from TAST. TAST-N is optimization-free and has the same support set configuration as T3A. T3A uses the prototype-based prediction of the test data itself, whereas TAST-N uses the aggregated predicted class distribution of the nearby support examples. As shown in Table 3, the prediction using the nearby support examples leads to a performance gain of 0.43% on average.

Effects of projection heads To understand the effect of projection heads, we test TAST with a varying number of projection heads, e.g., $N_e \in \{1, 5, 10, 20\}$. In Table 3, we find that utilizing a single projection head leads to degraded performance than TAST-N. However, TAST with multiple projection heads shows improvement over TAST-N and T3A on average.

4.2 Image Corruption

The image corruption benchmark is designed to evaluate the robustness to an unseen corrupted test domain of a classifier learned on a clean training domain. We use the publicly released code <https://github.com/vita-epfl/ttt-plus-plus> for the image corruption benchmark.

4.2.1 Experimental setup

We test robustness of TAST to image corruption on CIFAR-10 [26]. The CIFAR-10 dataset is composed of generic images consisting of a training and a test dataset with 50000 and 10000 examples of 10 classes, respectively. To make a corrupted test dataset, we apply 15 types of common image corruptions (e.g., Gaussian noise, shot noise) to the test dataset. We call the corrupted dataset CIFAR-10C [19]. We use the highest level (i.e., level-5) of image corruption for this experiment.

We use ResNet-50 as a backbone network. The method to train the network is different from the domain generalization benchmarks in Section 4.1. We train the network for 1000 epochs on the classification and instance discrimination tasks [4] jointly. For a fair comparison, we use the released trained model of [34] and the same hyperparameters whenever possible. We set the batch size to 128. We use Adam optimizer with a learning rate of 0.001 for test-time adaptation. The number of nearby support examples N_s is set to 1, the number of iterations per adaptation T is set to 1, the number of projection heads N_e is set to 20, and the number of support examples per each class M is set to 100. For TAST-BN, we restrict the size of the whole support set to 200. We run experiments using four different random seeds. More experimental results on other combinations of hyperparameters are summarized in Appendix C.

Table 4: Average error rate (%) on CIFAR-10C. **Bold** indicates the best performance for each image corruption. TAST-BN outperforms all the test-time adaptation methods and the state-of-the-art method TTT++ on most of experiments using different image corruptions.

Method	gauss	brit	contr	defoc	elast	fog	frost	glass	impul	jpeg	motn	pixel	shot	snow	zoom
No adaptation	48.73	7.01	13.27	11.84	23.38	29.41	28.24	50.78	57.00	19.46	23.38	47.88	44.00	21.93	10.84
+SHOT	17.09	8.64	8.57	9.83	19.53	19.72	13.93	25.60	27.15	13.98	14.01	11.68	16.02	15.89	8.22
+Tent	15.91	7.91	7.85	9.27	18.13	16.45	12.62	23.48	24.52	13.19	12.70	10.93	14.59	14.06	7.68
+PL	33.56	7.54	11.53	10.60	20.21	23.86	21.78	38.36	43.64	16.88	18.72	29.83	30.43	18.75	9.43
+T3A	41.87	7.30	13.61	11.99	22.06	28.52	27.13	44.10	54.26	18.71	22.54	37.53	37.84	21.97	10.72
+TAST (Ours)	42.02	7.34	13.55	11.86	21.38	28.58	26.51	44.99	54.19	18.96	22.55	37.08	37.62	21.84	10.64
+TAST-BN (Ours)	14.91	7.68	7.81	8.62	16.81	15.10	12.25	21.82	22.54	12.38	11.67	10.34	13.77	12.99	7.57
+TTT++	16.25	7.27	7.46	9.12	18.17	17.72	12.36	25.74	26.43	13.13	12.85	11.38	15.02	14.40	7.59

4.2.2 Experimental results

The overall experimental results on CIFAR-10C are summarized in Table 4. We observe that TAST improves the performance of the trained classifier by 2.54% on average. However, it is a minor improvement against the baseline methods, which fine-tune the feature extractor. On the other hand, TAST-BN outperforms all the test-time adaptation methods.

Additionally, we compare our method with the online version of TTT++ [34], which is one of the state-of-the-art methods on CIFAR-10C. TTT++ is one of the test-time training methods, which fine-tunes the feature extractor using the instance discrimination task along with matching the feature statistics of training and test time. As shown in Table 4, TAST-BN outperforms TTT++ in 13 out of 15 experiments using different image corruptions and achieves better performance by 1.24% on average. More experimental results in the offline setting are summarized in Appendix C.

5 Related works

Test-time training Test-time training methods [34, 47] fine-tune trained classifiers using the self-supervised learning task used at training time. Sun et al. [47] uses a rotation prediction task [13], which predicts the rotation angle of the rotated images. Liu et al. [34] use an instance discrimination task [4], which regards each image and its augmented images as a single class and discriminates against several classes. Test-time training methods have access to self-supervised learning tasks used at training time, whereas test-time adaptation methods, our focus in this paper, have no access to any information related to the training procedure.

Source-free domain adaptation Source-Free Domain Adaptation (SFDA) methods [9, 21, 32, 48, 61, 62] aim to adapt trained classifiers to unseen test domains without training dataset. Recently, several SFDA methods using nearest neighbor information [48, 61] have achieved good performances in domain adaptation benchmarks. SFDA methods mainly focus on the setting that they can access the whole unlabeled test data, whereas test-time adaptation methods focus on the setting that they can access the online unlabeled test data only.

6 Conclusion

We propose TAST to effectively adapt trained classifiers during test time using pseudo labels considering nearest neighbor information. Our method outperforms the state-of-the-art test-time adaptation methods on domain generalization and image corruption benchmarks. We expect our pseudo labeling method to be applied to other fields that utilize unlabeled data such as representation learning or few-shot learning. To the best of our knowledge, our work is the first one that utilizes an ensemble scheme for test-time adaptation. We expect that adaptation using the ensemble scheme can be combined with the other methods in source-free domain adaptation or test-time training.

One of the limitations of our method is that it requires huge memory if the number of classes or support examples per class is large. Especially for TAST-BN, the whole support set should be limited since the support examples are fed into the classifier together with the test data. This limitation should be addressed when applying our method to the problems dealing with larger datasets.

References

- [1] E. Arazo, D. Ortego, P. Albert, N. E. O’Connor, and K. McGuinness. Pseudo-labeling and confirmation bias in deep semi-supervised learning, 2020.
- [2] S. Beery, G. Van Horn, and P. Perona. Recognition in terra incognita. In *Proceedings of the European Conference on Computer Vision (ECCV)*, September 2018.
- [3] M. Caron, P. Bojanowski, A. Joulin, and M. Douze. Deep clustering for unsupervised learning of visual features. In *European Conference on Computer Vision*, 2018.
- [4] T. Chen, S. Kornblith, M. Norouzi, and G. Hinton. A simple framework for contrastive learning of visual representations. In H. D. III and A. Singh, editors, *Proceedings of the 37th International Conference on Machine Learning*, volume 119 of *Proceedings of Machine Learning Research*, pages 1597–1607. PMLR, 13–18 Jul 2020.
- [5] M. J. Choi, J. J. Lim, A. Torralba, and A. S. Willsky. Exploiting hierarchical context on a large database of object categories. In *2010 IEEE Computer Society Conference on Computer Vision and Pattern Recognition*, pages 129–136, 2010. doi: 10.1109/CVPR.2010.5540221.
- [6] K. Cobbe, O. Klimov, C. Hesse, T. Kim, and J. Schulman. Quantifying generalization in reinforcement learning. In K. Chaudhuri and R. Salakhutdinov, editors, *Proceedings of the 36th International Conference on Machine Learning*, volume 97 of *Proceedings of Machine Learning Research*, pages 1282–1289. PMLR, 09–15 Jun 2019.
- [7] G. Csurka. Domain adaptation for visual applications: A comprehensive survey. *CoRR*, abs/1702.05374, 2017.
- [8] D. Dwibedi, Y. Aytar, J. Tompson, P. Sermanet, and A. Zisserman. With a little help from my friends: Nearest-neighbor contrastive learning of visual representations. *CoRR*, abs/2104.14548, 2021.
- [9] C. Eastwood, I. Mason, C. Williams, and B. Schölkopf. Source-free adaptation to measurement shift via bottom-up feature restoration. In *International Conference on Learning Representations*, 2022.
- [10] M. Everingham, L. Gool, C. K. Williams, J. Winn, and A. Zisserman. The pascal visual object classes (voc) challenge. *Int. J. Comput. Vision*, 88(2):303–338, jun 2010. ISSN 0920-5691. doi: 10.1007/s11263-009-0275-4.
- [11] C. Fang, Y. Xu, and D. N. Rockmore. Unbiased metric learning: On the utilization of multiple datasets and web images for softening bias. In *2013 IEEE International Conference on Computer Vision*, pages 1657–1664, 2013. doi: 10.1109/ICCV.2013.208.
- [12] L. Fei-Fei, R. Fergus, and P. Perona. Learning generative visual models from few training examples: An incremental bayesian approach tested on 101 object categories. *Comput. Vis. Image Underst.*, 106(1):59–70, apr 2007. ISSN 1077-3142. doi: 10.1016/j.cviu.2005.09.012.
- [13] Z. Feng, C. Xu, and D. Tao. Self-supervised representation learning by rotation feature decoupling. In *2019 IEEE/CVF Conference on Computer Vision and Pattern Recognition (CVPR)*, pages 10356–10366, 2019. doi: 10.1109/CVPR.2019.01061.
- [14] Y. Ganin and V. Lempitsky. Unsupervised domain adaptation by backpropagation. In F. Bach and D. Blei, editors, *Proceedings of the 32nd International Conference on Machine Learning*, volume 37 of *Proceedings of Machine Learning Research*, pages 1180–1189, Lille, France, 07–09 Jul 2015. PMLR.
- [15] I. Gulrajani and D. Lopez-Paz. In search of lost domain generalization. In *International Conference on Learning Representations*, 2021.
- [16] C. Guo, G. Pleiss, Y. Sun, and K. Q. Weinberger. On calibration of modern neural networks. In D. Precup and Y. W. Teh, editors, *Proceedings of the 34th International Conference on Machine Learning*, volume 70 of *Proceedings of Machine Learning Research*, pages 1321–1330. PMLR, 06–11 Aug 2017.

- [17] K. He, X. Zhang, S. Ren, and J. Sun. Delving deep into rectifiers: Surpassing human-level performance on imagenet classification. In *2015 IEEE International Conference on Computer Vision (ICCV)*, pages 1026–1034, 2015. doi: 10.1109/ICCV.2015.123.
- [18] K. He, X. Zhang, S. Ren, and J. Sun. Deep residual learning for image recognition. In *2016 IEEE Conference on Computer Vision and Pattern Recognition (CVPR)*, pages 770–778, 2016. doi: 10.1109/CVPR.2016.90.
- [19] D. Hendrycks and T. Dietterich. Benchmarking neural network robustness to common corruptions and perturbations. *Proceedings of the International Conference on Learning Representations*, 2019.
- [20] A. Iscen, G. Toliás, Y. Avrithis, and O. Chum. Label propagation for deep semi-supervised learning. *2019 IEEE/CVF Conference on Computer Vision and Pattern Recognition (CVPR)*, pages 5065–5074, 2019.
- [21] M. Ishii and M. Sugiyama. Source-free domain adaptation via distributional alignment by matching batch normalization statistics. *ArXiv*, abs/2101.10842, 2021.
- [22] Y. Iwasawa and Y. Matsuo. Test-time classifier adjustment module for model-agnostic domain generalization. In M. Ranzato, A. Beygelzimer, Y. Dauphin, P. Liang, and J. W. Vaughan, editors, *Advances in Neural Information Processing Systems*, volume 34, pages 2427–2440. Curran Associates, Inc., 2021.
- [23] M. Jia, B. Chen, Z. Wu, C. Cardie, S. J. Belongie, and S. Lim. Rethinking nearest neighbors for visual classification. *CoRR*, abs/2112.08459, 2021.
- [24] M. Kaya and H. Ş. Bilge. Deep metric learning: A survey. *Symmetry*, 11(9):1066, 2019.
- [25] D. P. Kingma and J. Ba. Adam: A method for stochastic optimization, 2014. cite arxiv:1412.6980Comment: Published as a conference paper at the 3rd International Conference for Learning Representations, San Diego, 2015.
- [26] A. Krizhevsky and G. Hinton. Learning multiple layers of features from tiny images. Technical Report 0, University of Toronto, Toronto, Ontario, 2009.
- [27] A. Kumar, A. Raghunathan, R. M. Jones, T. Ma, and P. Liang. Fine-tuning can distort pre-trained features and underperform out-of-distribution. In *International Conference on Learning Representations*, 2022.
- [28] D.-H. Lee. Pseudo-label : The simple and efficient semi-supervised learning method for deep neural networks. *ICML 2013 Workshop : Challenges in Representation Learning (WREPL)*, 07 2013.
- [29] S. Lee and S.-Y. Chung. Improving generalization in meta-rl with imaginary tasks from latent dynamics mixture. In M. Ranzato, A. Beygelzimer, Y. Dauphin, P. Liang, and J. W. Vaughan, editors, *Advances in Neural Information Processing Systems*, volume 34, pages 27222–27235. Curran Associates, Inc., 2021.
- [30] D. Li, Y. Yang, Y. Song, and T. M. Hospedales. Deeper, broader and artier domain generalization. In *IEEE International Conference on Computer Vision, ICCV 2017, Venice, Italy, October 22-29, 2017*, pages 5543–5551. IEEE Computer Society, 2017. doi: 10.1109/ICCV.2017.591.
- [31] H. Li, S. J. Pan, S. Wang, and A. C. Kot. Domain generalization with adversarial feature learning. In *Proceedings of the IEEE Conference on Computer Vision and Pattern Recognition (CVPR)*, June 2018.
- [32] J. Liang, D. Hu, and J. Feng. Do we really need to access the source data? source hypothesis transfer for unsupervised domain adaptation. In *International Conference on Machine Learning (ICML)*, pages 6028–6039, 2020.
- [33] J. Lin. Divergence measures based on the shannon entropy. *IEEE Transactions on Information Theory*, 37(1):145–151, Jan. 1991. ISSN 0018-9448. doi: 10.1109/18.61115.

- [34] Y. Liu, P. Kothari, B. van Delft, B. Bellot-Gurlet, T. Mordan, and A. Alahi. Ttt++: When does self-supervised test-time training fail or thrive? In M. Ranzato, A. Beygelzimer, Y. Dauphin, P. Liang, and J. W. Vaughan, editors, *Advances in Neural Information Processing Systems*, volume 34, pages 21808–21820. Curran Associates, Inc., 2021.
- [35] M. Long, H. Zhu, J. Wang, and M. I. Jordan. Unsupervised domain adaptation with residual transfer networks. In D. Lee, M. Sugiyama, U. Luxburg, I. Guyon, and R. Garnett, editors, *Advances in Neural Information Processing Systems*, volume 29. Curran Associates, Inc., 2016.
- [36] R. Mendonca, X. Geng, C. Finn, and S. Levine. Meta-reinforcement learning robust to distributional shift via model identification and experience relabeling. *CoRR*, abs/2006.07178, 2020.
- [37] Y. Mesbah, Y. Y. Ibrahim, and A. M. Khan. Domain generalization using ensemble learning. *CoRR*, abs/2103.10257, 2021.
- [38] S. Motiian, M. Piccirilli, D. A. Adjeroh, and G. Doretto. Unified deep supervised domain adaptation and generalization. In *Proceedings of the IEEE International Conference on Computer Vision (ICCV)*, Oct 2017.
- [39] J. Mukhoti, V. Kulharia, A. Sanyal, S. Golodetz, P. Torr, and P. Dokania. Calibrating deep neural networks using focal loss. In H. Larochelle, M. Ranzato, R. Hadsell, M. Balcan, and H. Lin, editors, *Advances in Neural Information Processing Systems*, volume 33, pages 15288–15299. Curran Associates, Inc., 2020.
- [40] C. Rosenberg, M. Hebert, and H. Schneiderman. Semi-supervised self-training of object detection models. *2005 Seventh IEEE Workshops on Applications of Computer Vision (WACV/MOTION’05) - Volume 1*, 1:29–36, 2005.
- [41] B. Russell, A. Torralba, K. Murphy, and W. Freeman. Labelme: A database and web-based tool for image annotation. *International Journal of Computer Vision*, 77(1-3):157–173, 2008. ISSN 0920-5691. doi: 10.1007/s11263-007-0090-8.
- [42] K. Saenko, B. Kulis, M. Fritz, and T. Darrell. Adapting visual category models to new domains. In *Proceedings of the 11th European Conference on Computer Vision: Part IV, ECCV’10*, page 213–226, Berlin, Heidelberg, 2010. Springer-Verlag. ISBN 364215560X.
- [43] O. Sener, H. O. Song, A. Saxena, and S. Savarese. Learning transferrable representations for unsupervised domain adaptation. In D. Lee, M. Sugiyama, U. Luxburg, I. Guyon, and R. Garnett, editors, *Advances in Neural Information Processing Systems*, volume 29. Curran Associates, Inc., 2016.
- [44] J. Snell, K. Swersky, and R. Zemel. Prototypical networks for few-shot learning. In I. Guyon, U. V. Luxburg, S. Bengio, H. Wallach, R. Fergus, S. Vishwanathan, and R. Garnett, editors, *Advances in Neural Information Processing Systems*, volume 30. Curran Associates, Inc., 2017.
- [45] K. Sohn, D. Berthelot, C.-L. Li, Z. Zhang, N. Carlini, E. D. Cubuk, A. Kurakin, H. Zhang, and C. Raffel. Fixmatch: Simplifying semi-supervised learning with consistency and confidence. *arXiv preprint arXiv:2001.07685*, 2020.
- [46] B. Sun and K. Saenko. Deep CORAL: correlation alignment for deep domain adaptation. *CoRR*, abs/1607.01719, 2016.
- [47] Y. Sun, X. Wang, L. Zhuang, J. Miller, M. Hardt, and A. A. Efros. Test-time training with self-supervision for generalization under distribution shifts. In *ICML*, 2020.
- [48] S. Tang, Y. Yang, Z. Ma, N. Hendrich, F. Zeng, S. S. Ge, C. Zhang, and J. Zhang. Nearest neighborhood-based deep clustering for source data-absent unsupervised domain adaptation. *CoRR*, abs/2107.12585, 2021.
- [49] R. Taori, A. Dave, V. Shankar, N. Carlini, B. Recht, and L. Schmidt. Measuring robustness to natural distribution shifts in image classification. In H. Larochelle, M. Ranzato, R. Hadsell, M. Balcan, and H. Lin, editors, *Advances in Neural Information Processing Systems*, volume 33, pages 18583–18599. Curran Associates, Inc., 2020.

- [50] E. Tzeng, J. Hoffman, T. Darrell, and K. Saenko. Simultaneous deep transfer across domains and tasks. In *ICCV*, 2015.
- [51] H. Venkateswara, J. Eusebio, S. Chakraborty, and S. Panchanathan. Deep hashing network for unsupervised domain adaptation. *2017 IEEE Conference on Computer Vision and Pattern Recognition (CVPR)*, pages 5385–5394, 2017.
- [52] O. Vinyals, C. Blundell, T. Lillicrap, k. kavukcuoglu, and D. Wierstra. Matching networks for one shot learning. In D. Lee, M. Sugiyama, U. Luxburg, I. Guyon, and R. Garnett, editors, *Advances in Neural Information Processing Systems*, volume 29. Curran Associates, Inc., 2016.
- [53] D. Wang, E. Shelhamer, S. Liu, B. Olshausen, and T. Darrell. Tent: Fully test-time adaptation by entropy minimization. In *International Conference on Learning Representations*, 2021.
- [54] J. Wang, C. Lan, C. Liu, Y. Ouyang, and T. Qin. Generalizing to unseen domains: A survey on domain generalization. In Z.-H. Zhou, editor, *Proceedings of the Thirtieth International Joint Conference on Artificial Intelligence, IJCAI-21*, pages 4627–4635. International Joint Conferences on Artificial Intelligence Organization, 8 2021. doi: 10.24963/ijcai.2021/628. Survey Track.
- [55] Y. Wang, X. Xu, H. Zhao, and Z. Hua. Semi-supervised learning based on nearest neighbor rule and cut edges. *Knowledge-Based Systems*, 23:547–554, 08 2010. doi: 10.1016/j.knosys.2010.03.012.
- [56] Y. Wang, W.-L. Chao, K. Q. Weinberger, and L. van der Maaten. Simpleshot: Revisiting nearest-neighbor classification for few-shot learning. *arXiv preprint arXiv:1911.04623*, 2019.
- [57] Y. Wen, D. Tran, and J. Ba. Batchensemble: an alternative approach to efficient ensemble and lifelong learning. In *International Conference on Learning Representations*, 2020.
- [58] Q. Xie, M.-T. Luong, E. Hovy, and Q. V. Le. Self-training with noisy student improves imagenet classification. In *Proceedings of the IEEE/CVF Conference on Computer Vision and Pattern Recognition (CVPR)*, June 2020.
- [59] M. Xu, J. Zhang, B. Ni, T. Li, C. Wang, Q. Tian, and W. Zhang. Adversarial domain adaptation with domain mixup. In *The Thirty-Fourth AAAI Conference on Artificial Intelligence*, pages 6502–6509. AAAI Press, 2020.
- [60] L. Yang and R. Jin. Distance metric learning: A comprehensive survey. *Michigan State University*, 2, 2006.
- [61] S. Yang, Y. Wang, J. van de weijer, L. Herranz, and S. JUI. Exploiting the intrinsic neighborhood structure for source-free domain adaptation. In A. Beygelzimer, Y. Dauphin, P. Liang, and J. W. Vaughan, editors, *Advances in Neural Information Processing Systems*, 2021.
- [62] H.-W. Yeh, B. Yang, P. C. Yuen, and T. Harada. Sofa: Source-data-free feature alignment for unsupervised domain adaptation. In *2021 IEEE Winter Conference on Applications of Computer Vision (WACV)*, pages 474–483, 2021. doi: 10.1109/WACV48630.2021.00052.
- [63] A. YM., R. C., and V. A. Self-labelling via simultaneous clustering and representation learning. In *International Conference on Learning Representations*, 2020.

1. For all authors...
 - (a) Do the main claims made in the abstract and introduction accurately reflect the paper's contributions and scope? [Yes]
 - (b) Did you describe the limitations of your work? [Yes] See Section 6
 - (c) Did you discuss any potential negative societal impacts of your work? [N/A]
 - (d) Have you read the ethics review guidelines and ensured that your paper conforms to them? [Yes]
2. If you are including theoretical results...
 - (a) Did you state the full set of assumptions of all theoretical results? [N/A]
 - (b) Did you include complete proofs of all theoretical results? [N/A]
3. If you ran experiments...
 - (a) Did you include the code, data, and instructions needed to reproduce the main experimental results (either in the supplemental material or as a URL)? [Yes] See Section 4
 - (b) Did you specify all the training details (e.g., data splits, hyperparameters, how they were chosen)? [Yes] See Section 4 and Appendix
 - (c) Did you report error bars (e.g., with respect to the random seed after running experiments multiple times)? [Yes]
 - (d) Did you include the total amount of compute and the type of resources used (e.g., type of GPUs, internal cluster, or cloud provider)? [Yes] See Appendix
4. If you are using existing assets (e.g., code, data, models) or curating/releasing new assets...
 - (a) If your work uses existing assets, did you cite the creators? [Yes]
 - (b) Did you mention the license of the assets? [Yes] See the source codes in the supplementary material
 - (c) Did you include any new assets either in the supplemental material or as a URL? [Yes] See the source codes in the supplementary material
 - (d) Did you discuss whether and how consent was obtained from people whose data you're using/curating? [N/A]
 - (e) Did you discuss whether the data you are using/curating contains personally identifiable information or offensive content? [N/A]
5. If you used crowdsourcing or conducted research with human subjects...
 - (a) Did you include the full text of instructions given to participants and screenshots, if applicable? [N/A]
 - (b) Did you describe any potential participant risks, with links to Institutional Review Board (IRB) approvals, if applicable? [N/A]
 - (c) Did you include the estimated hourly wage paid to participants and the total amount spent on participant compensation? [N/A]

A Implementation Details

A.1 Implementation details on domain generalization benchmarks

We follow the dataset splits and the hyperparameter selection method used in T3A. We split each dataset of training domains into training and validation sets. The training and validation sets are used for network training and hyperparameter selection, respectively. Specifically, we split each dataset into 80% and 20% and use the smaller set as the validation set. We choose the hyperparameters that maximize the validation accuracy of the adapted classifier. This hyperparameter selection method is called the training-domain validation. We train backbone networks using four different learning algorithms: ERM, CORAL, MMD, and Mixup. ERM is explained in Section 2 of the main paper; CORAL aims to obtain domain-invariant representations by aligning covariance matrices of training data and test data; MMD tries to match the training and test data distributions using the MMD measure; Mixup trains classifiers using mixed images/features and mixed labels created by linear interpolation of examples from the training domains. We run experiments using four different random seeds: 0, 1, 2, and 3.

All the hyperparameters for training and test-time adaptation are taken from T3A and DomainBed. We train the network with Adam optimizer with default hyperparameters introduced in DomainBed, e.g., a learning rate of 0.00005, a weight decay of 0, a dropout rate of 0, and a batch size of 32. In addition to the hyperparameters for test-time adaptation described in Section 4.1.1 of the main paper, there is one more hyperparameter β for the baseline methods. The learning rate for test-time adaptation is obtained by multiplying β to the learning rate used in training time. The possible values for β are set to 0.1, 1.0, and 10.0.

A.2 Implementation details on image corruption benchmark

We use the same hyperparameters introduced in TTT++. We train ResNet-50 for 1000 epochs using the classification and instance discrimination tasks jointly. The weight on the instance discrimination task for balancing the two tasks is set to 0.1. For the instance discrimination task, we use the same data augmentation schemes of TTT++, e.g., RandomResizeCrop, RandomHorizontalCrop, HorizontalFlip, ColorJitter, RandomGrayscale, and Normalization. We set the batch size for training the networks to 256. At test time, PL, SHOT, and TTT++ use SGD optimizer with a learning rate of 0.001 and a momentum of 0.9. On the other hand, Tent, TAST, and TAST-BN use Adam optimizer with a learning rate of 0.001. We set the batch size to 128 during the test time due to effective memory usage. We run experiments using four different random seeds: 0, 1, 2, and 3.

A.3 Runtime comparison

Table 5: Mean runtime to adapt classifiers that use ResNet-18 as a backbone network.

Method	VLCS	PACS	OfficeHome	TerraIncognita
Tent	7m 28s	3m 16s	7m 25s	10m 34s
TentBN	2m 8s	33s	1m 57s	2m 58s
TentClf	2m 7s	34s	1m 57s	2m 56s
SHOT	8m 9s	4m 22s	8m 38s	12m 40s
SHOTIM	8m 8s	4m 19s	8m 35s	12m 35s
PL	8m 18s	4m 43s	8m 43s	12m 55s
PLClf	2m 7s	35s	1m 59s	2m 57s
T3A	2m 9s	33s	2m 15s	2m 59s
TAST (Ours)	10m 34s	9m 30s	22m 24s	26m 14s
TAST-BN (Ours)	18m 43s	16m 32s	38m 27s	45m 5s

We conduct our experiments on TITAN XP. We report the average runtime spent to adapt classifiers that use ResNet-18 as a backbone network in Table 5. T3A is one of the algorithms having the least running time since it is optimization-free. TentBN, TentClf, and PLClf also require less running time. These methods fine-tune only the small parts of the trained classifier such as the last linear classifier or the attached BN layer. On the other hand, TAST and TAST-BN require more running time since they retrieve the nearest neighbors in the embedding space for each test sample.

Algorithm 2 TAST-BN

Require: Feature extractor f_θ , test batch \mathbb{B} , support set \mathbb{S} , number of iterations per adaptation T , number of support examples per each class M , number of nearby support examples N_s , learning rate α

Ensure: Predictions \hat{y}_x for all $x \in \mathbb{B}$

Update the support set \mathbb{S} with eq. (11) in Section B

Retrieve the nearest neighbors $\mathcal{N}\mathcal{N}(x; \mathbb{S})$ for all $x \in \mathbb{B}$ with eq. (12) in Section B

for $t = 1 : T$ **do**

 Compute prototypes $\{\mu_k\}_{k=1}^K$ using the support set in the embedding space of f_θ

for $z \in \mathcal{N}\mathcal{N}(x; \mathbb{S})$ **do**

$$p^{\text{proto}}(k|z) \leftarrow \frac{\exp(-d(f_\theta(z), \mu_k)/\tau)}{\sum_c \exp(-d(f_\theta(z), \mu_c)/\tau)}, k = 1, 2, \dots, K$$

end for

for $x \in \mathbb{B}$ **do**

$$\hat{p}^{\text{TAST}}(k|x) \leftarrow \frac{1}{N_s} \sum_{z \in \mathcal{N}\mathcal{N}(x; \mathbb{S})} \mathbb{1}[\arg \max_c p^{\text{proto}}(c|z) = k], k = 1, 2, \dots, K$$

$$p^{\text{proto}}(k|x) \leftarrow \frac{\exp(-d(f_\theta(x), \mu_k)/\tau)}{\sum_c \exp(-d(f_\theta(x), \mu_c)/\tau)}, k = 1, 2, \dots, K$$

end for

$$\theta \leftarrow \theta - \alpha \nabla_\theta \frac{1}{|\mathbb{B}|} \sum_{x \in \mathbb{B}} \text{CE}(\hat{p}^{\text{TAST}}(Y|x), p^{\text{proto}}(Y|x))$$

end for

for $x \in \mathbb{B}$ **do**

$$p^{\text{TAST}}(k|x) \leftarrow \frac{1}{N_s} \sum_{z \in \mathcal{N}\mathcal{N}(x; \mathbb{S})} p^{\text{proto}}(k|z), k = 1, 2, \dots, K$$

$$\hat{y}_x \leftarrow \arg \max_c p^{\text{TAST}}(c|x)$$

end for

B Pseudocode for TAST-BN

We present the pseudocode for TAST-BN in Algorithm 2. TAST-BN fine-tunes the BN layers in the feature extractor instead of projection heads. Since the embedding space of the feature extractor steadily changes, the support set stores the test data itself instead of the feature representations. Formally, a support set $\mathbb{S}_t = \{\mathbb{S}_t^1, \mathbb{S}_t^2, \dots, \mathbb{S}_t^K\}$ is a set of test samples until time t . The support set is initialized as an empty set. At the time t , the support set is updated as

$$\mathbb{S}_t^k = \begin{cases} \mathbb{S}_{t-1}^k \cup \{x_t\}, & \text{if } \arg \max_c p_c = k \\ \mathbb{S}_{t-1}^k, & \text{otherwise,} \end{cases} \quad (11)$$

where p_k is the likelihood the classifier assigns x_t to the class k . Using the support set, we retrieve N_s nearby support examples of x in the embedding space of f_θ , i.e.,

$$\mathcal{N}\mathcal{N}(x; \mathbb{S}) := \{z \in \mathbb{S} | d(f_\theta(x), f_\theta(z)) \leq \beta_x\}, \quad (12)$$

where β_x is the distance between x and the N_s -th nearest neighbor of x from \mathbb{S} in the embedding space of f_θ . Then, we generate a pseudo label for the test data and fine-tune the BN layers to predict the pseudo label for the test data with the same procedure described in Section 3 of the main paper.

C Additional Experiments

C.1 Fine-tuning both projection heads and BN layers simultaneously

We consider a method, named TAST-both, that fine-tunes both the attached projection heads and the BN layers in the feature extractor simultaneously. Table 6 reports the experimental results using classifiers learned by ERM on domain generalization benchmarks. We use ResNet-18 as a backbone network. As shown in Table 6, TAST-both shows worse performance than TAST-BN and TAST. We conjecture that the random initialization of projection heads and the changes in feature representation due to BN layer training negatively affect the learning of the other layers.

C.2 Experimental results using different hyperparameters on CIFAR-10C

In Table 4 of the main paper, we report the experimental results when N_s and M are set to 1 and 100 on the CIFAR-10C, respectively. In Table 7, we summarize the experimental results using different combinations of N_s and M on the CIFAR-10C. There are two observations in Table 7 that (1) T3A has shown the best performances when M is set to 100, and (2) TAST and TAST-BN perform better with smaller N_s .

Table 6: Average accuracy (%) using classifiers trained by ERM on domain generalization benchmarks. We use ResNet-18 as a backbone network. TAST-both is a method fine-tunes both the attached projection heads and the BN layers simultaneously. TAST-both shows worse performances than TAST-BN and TAST.

Method	N_e	VLCS	PACS	OfficeHome	TerraIncognita	avg
ERM	-	74.88±0.46	79.30±0.77	62.09±0.31	40.63±1.19	64.22
+T3A	-	77.26±1.49	80.83±0.67	63.21±0.50	40.20±0.60	65.38
+TAST-N	-	76.20±1.87	81.62±0.52	63.54±0.63	41.88±1.21	65.81
+TAST-BN	-	75.21±2.36	87.07±0.53	62.79±0.41	39.43±2.24	66.13
+TAST	1	75.20±0.77	81.23±0.70	62.09±0.64	42.59±0.41	65.28
	5	76.68±0.77	81.81±0.13	63.51±0.59	42.68±0.80	66.17
	10	77.43±0.62	81.56±0.85	63.39±0.56	42.60±0.63	66.25
	20	77.27±0.67	81.94±0.44	63.70±0.52	42.64±0.72	66.39
+TAST-both	1	73.35±0.57	84.85±0.56	61.70±0.39	39.27±2.05	64.79
	5	73.88±0.35	84.99±0.63	61.81±0.44	39.16±1.57	64.96
	10	73.66±1.57	85.13±0.27	62.03±0.52	38.50±1.25	64.83
	20	75.16±0.17	85.52±0.05	62.01±0.67	38.54±1.52	65.31

Table 7: Average error rate (%) in the online setting on CIFAR-10C with different hyperparameters.

Method	M	N_e	gauss	brit	contr	defoc	elast	fog	frost	glass	impul	jpeg	motn	pixel	shot	snow	zoom
No adaptation	-	-	48.73	7.01	13.27	11.84	23.38	29.41	28.24	50.78	57.00	19.46	23.38	47.88	44.00	21.93	10.84
+T3A	1	-	44.56	8.28	13.27	13.45	22.18	28.59	27.18	46.43	55.11	18.96	22.59	42.92	40.32	21.77	10.53
+T3A	5	-	44.65	7.94	14.11	13.34	22.67	29.00	28.57	45.92	56.03	19.67	24.16	40.18	40.55	22.61	12.02
+T3A	20	-	44.26	7.72	13.82	13.35	22.24	28.71	28.36	45.49	55.87	19.34	23.76	39.82	40.38	22.44	12.20
+T3A	50	-	42.82	7.43	13.65	12.36	22.15	28.54	27.69	44.42	54.91	19.13	22.83	38.33	38.53	22.09	11.15
+T3A	100	-	41.87	7.30	13.61	11.99	22.06	28.52	27.13	44.10	54.26	18.71	22.54	37.53	37.84	21.97	10.72
+T3A	-1	-	43.83	7.33	13.56	11.63	22.11	29.07	27.56	46.79	55.16	18.73	22.77	41.16	39.58	22.23	10.34
+TAST	1	1	47.24	8.68	12.93	16.74	22.31	28.66	27.23	48.76	55.97	19.21	22.63	48.32	42.80	21.57	10.34
+TAST	5	1	47.19	9.78	15.88	15.58	24.30	30.94	29.70	48.66	58.05	21.49	27.57	41.00	44.21	24.58	14.75
+TAST	5	2	48.08	11.34	17.73	17.10	25.93	31.99	30.54	49.77	58.54	23.72	29.55	44.09	45.55	26.23	16.41
+TAST	5	4	48.53	10.95	17.25	16.82	25.58	31.78	30.19	50.00	58.86	23.67	29.35	43.37	45.35	25.63	16.26
+TAST	20	1	43.58	7.74	14.01	12.97	21.90	28.73	27.76	45.62	55.20	19.78	23.63	38.77	39.22	22.73	12.13
+TAST	20	2	44.38	8.22	14.51	13.73	22.28	29.07	28.66	46.30	55.92	20.49	24.39	40.60	40.38	23.37	12.76
+TAST	20	4	44.41	8.19	14.26	13.60	22.22	29.05	28.81	46.17	56.05	20.09	24.24	40.33	40.39	23.18	12.67
+TAST	50	1	42.47	7.37	13.65	12.14	21.48	28.30	26.88	44.99	54.52	19.26	22.76	37.59	37.73	22.06	11.03
+TAST	50	2	42.79	7.62	14.11	12.30	21.57	28.73	27.50	45.26	55.18	19.96	23.10	38.99	38.43	22.43	11.25
+TAST	50	4	42.89	7.54	13.90	12.15	21.45	28.51	27.48	45.10	54.93	19.71	22.87	38.94	38.21	22.29	11.02
+TAST	100	1	42.02	7.34	13.55	11.86	21.38	28.58	26.51	44.99	54.19	18.96	22.55	37.08	37.62	21.84	10.64
+TAST	100	2	42.35	7.61	13.89	11.95	21.50	28.75	27.06	45.15	54.55	19.58	22.77	38.09	37.64	21.99	10.73
+TAST	100	4	42.34	7.50	13.80	11.72	21.45	28.32	26.89	44.75	54.46	19.18	22.54	38.00	37.61	21.97	10.67
+TAST	-1	1	45.20	7.44	14.05	11.55	22.87	30.19	27.87	50.28	57.07	19.65	22.95	41.99	41.35	22.65	10.20
+TAST	-1	2	44.86	7.45	13.88	11.62	22.03	29.38	28.03	50.37	58.25	20.02	22.73	42.67	41.04	22.48	10.30
+TAST	-1	4	44.93	7.36	13.64	11.17	21.57	28.82	28.17	49.63	58.74	19.64	22.41	43.38	41.02	22.15	9.86
+TAST-BN	1	1	19.46	11.95	11.02	12.84	21.54	19.38	16.64	26.03	27.76	17.93	15.29	14.01	19	17.94	11.78
+TAST-BN	5	1	16.21	8.4	8.48	9.56	17.92	15.59	13.06	23.1	23.68	13.58	12.79	11.06	14.85	14.02	8.36
+TAST-BN	5	2	17.26	9.27	9.23	10.51	19.51	16.17	13.86	24.32	24.69	14.57	13.81	12.05	15.98	15.06	8.95
+TAST-BN	5	4	18.89	10.29	11.05	13.23	20.66	16.99	14.79	24.95	26.1	16.12	17.02	13.57	18.42	17.11	10.22
+TAST-BN	20	1	14.91	7.68	7.81	8.62	16.81	15.10	12.25	21.82	22.54	12.38	11.67	10.34	13.77	12.99	7.57
+TAST-BN	20	2	15.11	7.85	7.96	8.75	17.00	15.02	12.32	22.07	22.54	12.57	11.99	10.50	13.98	13.12	7.70
+TAST-BN	20	4	15.00	7.98	8.00	8.71	16.87	14.89	12.24	21.88	22.43	12.55	11.89	10.47	14.06	13.06	7.59

C.3 Experimental results in the offline setting on CIFAR-10C

In Table 4 of the main paper, the experimental results of test-time adaptation methods are reported in the online setting on CIFAR-10C. In Table 8, we summarize the experimental results in the offline setting on CIFAR-10C. We follow the experimental setup described in the source code of TTT++. As shown in Table 8, TAST shows better performance than T3A by 1.31% on average. However, it is a minor improvement against the baseline methods, which fine-tune the feature extractor. On the other hand, TAST-BN outperforms all the baseline test-time adaptation methods and achieves competitive results with TTT++. Specifically, TAST-BN outperforms TTT++ in 7 out of 15 experiments using different image corruptions.

D Full Results

Table 8: Average error rate (%) in the offline setting on CIFAR-10C. **Bold** indicates the best performance for each benchmark. TAST-BN outperforms all the test-time adaptation methods and shows the competitive results compared to the state-of-the-art algorithm TTT++, which has access to self-supervised learning tasks used during training time.

Method	gauss	brit	contr	defoc	elast	fog	frost	glass	impul	jpeg	motn	pixel	shot	snow	zoom
SHOT	15.40	7.67	7.38	8.83	17.59	16.38	12.24	22.53	24.31	12.79	12.09	10.54	14.26	13.60	7.35
Tent	15.20	7.74	7.63	8.92	16.97	13.97	12.34	21.46	22.15	12.74	11.82	10.33	13.72	12.48	7.75
PL	55.98	6.96	12.02	11.41	21.87	26.74	26.30	48.53	77.52	18.50	21.72	45.46	47.77	21.08	9.99
T3A	42.50	7.42	13.62	12.34	22.20	28.21	27.63	44.41	54.93	19.12	22.68	37.35	38.43	22.05	11.10
TAST	41.58	7.21	13.22	11.84	21.28	28.29	26.83	44.06	53.87	18.91	22.77	36.11	37.06	21.63	10.62
TAST-BN	14.07	7.27	7.32	8.11	15.61	13.19	11.83	20.15	21.06	11.79	10.47	9.75	13.23	11.70	7.33
TTT++	14.67	6.12	6.54	9.14	14.71	10.10	11.54	18.42	11.97	12.41	10.60	10.09	13.34	11.05	8.38

Table 9: Full results using classifiers trained by ERM for Table 1 on VLCS. We use ResNet-18 as a backbone network.

Method	C	L	S	V	Avg
ERM	94.70±1.33	63.79±1.30	67.90±1.97	73.15±1.37	74.88
+Tent	89.82±2.89	61.98±1.10	65.51±1.91	74.21±1.61	72.88
+TentBN	79.80±4.74	58.51±1.44	61.62±0.92	68.14±1.74	67.02
+TentClf	94.75±1.43	63.74±1.41	67.92±2.22	65.40±6.91	72.96
+SHOT	91.45±6.83	48.26±1.77	54.75±2.59	66.51±1.25	65.24
+SHOTIM	90.28±7.00	47.96±1.45	54.66±2.47	66.52±1.19	64.86
+PL	93.57±2.24	53.82±2.51	50.58±9.50	53.91±2.78	62.97
+PLClf	94.67±1.38	63.64±1.31	67.90±2.21	73.34±1.00	74.89
+T3A	97.52±1.99	65.32±2.24	70.70±3.48	75.51±1.75	77.26
+TAST (Ours)	99.17±0.60	65.87±1.90	68.13±1.76	75.92±1.75	77.27
+TAST-BN (Ours)	92.60±8.66	64.75±1.29	67.27±3.14	76.23±3.73	75.21

Table 10: Full results using classifiers trained by ERM for Table 1 on PACS. We use ResNet-18 as a backbone network.

Method	A	C	P	S	Avg
ERM	77.78±0.81	75.09±1.22	95.19±0.29	69.11±1.22	79.29
+Tent	82.21±1.07	81.20±0.51	95.32±0.33	76.82±1.97	83.89
+TentBN	78.89±0.67	77.45±0.82	95.77±0.40	70.89±2.75	80.75
+TentClf	78.16±1.05	75.01±1.53	95.50±0.35	65.60±5.96	78.57
+SHOT	81.09±0.86	79.68±0.91	96.18±0.27	72.48±2.04	82.36
+SHOTIM	81.10±0.90	79.66±0.95	96.18±0.27	72.35±2.03	82.33
+PL	76.42±4.89	61.05±5.48	95.70±0.56	50.75±8.79	70.98
+PLClf	79.09±1.41	75.46±2.93	95.43±0.32	62.48±7.31	78.11
+T3A	78.81±0.97	77.14±1.20	95.92±0.36	71.44±1.63	80.83
+TAST (Ours)	80.56±0.53	78.26±0.99	96.44±0.20	72.52±0.77	81.94
+TAST-BN (Ours)	86.49±0.20	83.70±2.57	97.23±0.11	80.85±1.42	87.07

Table 11: Full results using classifiers trained by ERM for Table 1 on OfficeHome. We use ResNet-18 as a backbone network.

Method	A	C	P	R	Avg
ERM	55.19±0.49	47.76±1.02	72.22±0.53	73.21±0.89	62.10
+Tent	53.39±0.61	48.28±0.88	70.50±0.68	71.29±0.72	60.86
+TentBN	55.53±0.43	49.53±0.95	72.47±0.27	73.01±1.23	62.64
+TentClf	55.17±0.67	36.73±1.94	72.21±0.52	73.22±0.97	59.33
+SHOT	55.14±0.57	50.27±1.18	71.69±0.45	73.21±0.91	62.58
+SHOTIM	55.08±0.56	50.29±1.17	71.71±0.40	73.21±0.90	62.57
+PL	54.49±1.06	34.66±13.13	71.45±0.37	72.20±0.65	58.20
+PLClf	55.14±0.70	47.70±1.25	72.21±0.54	72.62±0.96	61.92
+T3A	55.10±0.74	49.56±1.14	74.10±0.55	74.07±1.18	63.21
+TAST (Ours)	56.15±0.68	50.04±1.31	74.33±0.28	74.28±1.23	63.70
+TAST-BN (Ours)	55.11±0.58	51.35±0.85	72.58±0.80	72.13±0.78	62.79

Table 12: Full results using classifiers trained by ERM for Table 1 on TerraIncognita. We use ResNet-18 as a backbone network.

Method	L100	L38	L43	L46	Avg
ERM	37.18±2.46	36.12±4.20	53.18±1.27	36.02±1.37	40.62
+Tent	38.29±0.48	25.82±3.91	41.53±1.59	29.15±1.83	33.70
+TentBN	40.55±1.46	37.44±2.22	46.33±1.32	35.30±1.26	39.91
+TentClf	34.44±13.31	34.19±5.76	52.71±2.03	31.86±2.26	38.30
+SHOT	33.87±0.66	28.58±2.10	40.99±2.07	30.83±1.26	33.57
+SHOTIM	33.83±1.29	28.13±2.30	40.81±2.18	30.64±1.46	33.35
+PL	51.92±1.19	35.61±20.74	39.97±10.98	22.26±8.21	37.44
+PLClf	45.22±2.45	36.03±5.81	52.76±1.54	33.10±2.27	41.78
+T3A	36.22±1.89	40.08±1.98	50.72±1.02	33.79±1.25	40.20
+TAST (Ours)	43.67±2.83	39.24±3.79	52.64±3.02	35.01±1.09	42.64
+TAST-BN (Ours)	51.06±7.31	32.74±7.54	41.70±2.86	32.21±3.05	39.43

Table 13: Full results using classifiers trained by ERM for Table 1 on VLCS. We use ResNet-50 as a backbone network.

Method	C	L	S	V	Avg
ERM	97.66±0.64	63.87±1.71	71.21±1.52	74.09±2.06	76.71
+Tent	92.36±2.44	58.46±3.29	67.84±2.03	73.19±2.68	72.96
+TentBN	85.36±3.49	58.35±3.46	66.47±2.71	68.42±2.11	69.65
+TentClf	97.61±0.58	63.67±2.10	68.77±1.27	73.16±1.31	75.80
+SHOT	98.72±1.50	46.82±2.57	55.70±1.78	67.04±2.88	67.07
+SHOTIM	98.65±1.46	46.54±2.32	55.81±2.32	66.73±2.82	66.93
+PL	98.48±0.34	53.45±2.82	59.45±9.24	66.24±8.63	69.41
+PLClf	97.63±0.64	63.36±2.10	69.74±0.78	71.86±4.53	75.65
+T3A	99.17±0.38	64.78±1.61	73.01±3.24	72.20±2.84	77.29
+TAST (Ours)	99.35±0.30	65.64±1.78	73.63±3.58	72.01±2.68	77.66
+TAST-BN (Ours)	96.09±2.40	60.22±6.08	65.78±6.51	71.99±5.90	73.52

Table 14: Full results using classifiers trained by ERM for Table 1 on PACS. We use ResNet-50 as a backbone network.

Method	A	C	P	S	Avg
ERM	82.92±1.65	78.05±3.36	96.50±0.32	75.38±3.31	83.21
+Tent	82.54±1.32	84.90±1.35	95.45±0.93	77.74±1.36	85.16
+TentBN	82.75±2.01	79.50±2.26	96.78±0.20	75.73±3.22	83.69
+TentClf	83.00±1.87	77.86±4.20	96.55±0.36	73.25±6.14	82.66
+SHOT	84.67±1.70	80.17±1.39	96.58±0.52	74.86±2.95	84.07
+SHOTIM	84.62±1.79	80.24±1.41	96.54±0.46	75.16±2.88	84.14
+PL	84.59±5.51	76.35±2.57	96.41±0.68	69.54±11.22	81.72
+PLClf	83.88±2.00	78.93±3.68	96.53±0.40	73.96±6.08	83.33
+T3A	83.56±2.03	79.75±3.14	96.99±0.24	75.36±3.57	83.92
+TAST (Ours)	83.85±2.05	79.15±3.03	96.93±0.27	76.49±3.13	84.11
+TAST-BN (Ours)	87.11±2.04	88.50±1.93	97.79±0.47	83.23±1.42	89.16

Table 15: Full results using classifiers trained by ERM for Table 1 on OfficeHome. We use ResNet-50 as a backbone network.

Method	A	C	P	R	Avg
ERM	61.32±0.69	53.44±1.11	75.84±1.10	77.90±0.92	67.13
+Tent	60.98±0.67	53.94±1.24	74.49±0.71	75.75±0.53	66.29
+TentBN	62.63±0.45	54.90±1.17	76.20±1.09	77.92±1.01	67.91
+TentClf	61.35±0.73	52.72±1.40	75.23±1.05	77.86±1.07	66.79
+SHOT	61.91±0.33	55.58±0.91	75.49±1.54	77.60±0.80	67.65
+SHOTIM	61.84±0.32	55.63±0.92	75.56±1.60	77.57±0.79	67.65
+PL	59.42±1.55	42.40±12.31	73.80±2.26	75.77±1.50	62.85
+PLClf	61.35±0.40	52.87±1.96	75.86±1.09	77.94±1.10	67.01
+T3A	61.91±0.59	55.07±1.14	77.39±1.38	78.67±0.61	68.26
+TAST (Ours)	62.43±0.80	55.81±1.26	77.46±1.07	78.83±0.93	68.63
+TAST-BN (Ours)	63.22±0.85	58.20±0.98	77.14±1.10	76.94±0.39	68.88

Table 16: Full results using classifiers trained by ERM for Table 1 on TerraIncognita. We use ResNet-50 as a backbone network.

Method	L100	L38	L43	L46	Avg
ERM	46.84±1.96	43.24±2.51	53.32±1.92	40.30±1.93	45.93
+Tent	41.20±2.71	29.72±3.59	41.35±2.92	36.03±2.85	37.08
+TentBN	46.64±1.17	41.11±3.16	49.31±1.05	38.52±2.04	43.89
+TentClf	49.87±3.80	43.31±3.19	53.01±2.31	28.40±6.19	43.64
+SHOT	36.17±2.70	29.80±2.92	41.00±0.30	33.83±1.86	35.20
+SHOTIM	35.56±2.76	27.49±4.01	40.77±0.45	33.67±1.84	34.37
+PL	56.75±5.78	46.12±1.03	29.44±10.14	20.06±4.65	38.09
+PLClf	52.28±3.95	43.76±2.96	52.78±2.15	37.81±2.49	46.66
+T3A	45.13±1.26	44.67±2.56	52.52±0.78	40.13±2.31	45.61
+TAST (Ours)	53.01±3.95	43.27±3.21	53.79±2.72	39.66±3.65	47.43
+TAST-BN (Ours)	55.75±2.37	33.92±9.86	43.87±4.70	32.33±4.40	41.47

Table 17: Average accuracy(%) using classifiers trained by CORAL on the domain generalization benchmarks for Table 2 of the main paper, namely VLCS, PACS, OfficeHome, and TerraIncognita. We use ResNet-18 and ResNet-50 as backbone networks. **Bold** indicates the best performance for each benchmark. Our proposed method TAST outperforms all the baselines on most of the benchmarks.

Method	Backbone	VLCS	PACS	OfficeHome	TerraIncognita	Avg	
CORAL	ResNet-18	74.00±1.13	81.00±0.79	62.78±0.06	36.51±2.35	63.57	
+Tent		71.13±1.45	84.17±0.61	62.37±0.09	36.71±0.77	63.60	
+TentBN		65.66±1.86	82.28±0.36	63.37±0.13	37.89±1.23	62.30	
+TentClf		72.27±1.29	75.71±1.74	62.65±0.08	30.27±6.34	60.23	
+SHOT		66.01±3.75	84.67±0.47	63.54±0.23	33.20±0.49	61.86	
+SHOTIM		65.75±3.70	84.63±0.49	63.53±0.21	33.10±0.42	61.75	
+PL		66.58±1.92	76.46±3.23	61.19±1.52	29.32±5.57	58.39	
+PLClf		73.70±0.39	76.16±2.44	62.68±0.13	34.29±3.96	61.71	
+T3A		75.49±1.67	82.75±0.51	63.72±0.32	38.39±1.39	65.09	
+TAST (Ours)		74.82±2.43	83.16±0.81	64.00±0.25	39.21±1.75	65.30	
+TAST-BN (Ours)		77.01±0.36	87.21±0.57	62.98±0.23	37.45±1.11	66.16	
CORAL		ResNet-50	76.39±1.01	83.52±0.67	66.89±0.20	42.79±1.27	67.40
+Tent			74.43±0.98	86.50±0.77	66.30±0.28	42.15±2.81	67.35
+TentBN			68.26±1.39	85.05±0.59	67.68±0.20	41.54±0.93	65.63
+TentClf	76.45±1.00		82.14±1.71	64.03±0.56	39.74±2.47	65.59	
+SHOT	64.11±0.79		85.09±1.03	67.73±0.29	33.96±0.59	62.72	
+SHOTIM	63.63±0.60		85.06±0.93	67.72±0.29	34.17±0.90	62.65	
+PL	72.74±1.32		75.96±6.46	60.74±2.91	36.69±3.47	61.53	
+PLClf	75.68±1.23		83.56±0.80	66.24±0.42	44.93±3.76	67.60	
+T3A	77.33±0.97		84.54±0.63	68.08±0.34	43.50±0.19	68.36	
+TAST (Ours)	77.23±1.25		85.04±0.49	68.39±0.54	44.22±1.33	68.72	
+TAST-BN (Ours)	79.13±0.43		90.41±0.64	69.04±0.36	43.46±4.46	70.51	

Table 18: Full results using classifiers trained by CORAL for Table 17 on VLCS. We use ResNet-18 as a backbone network.

Method	C	L	S	V	Avg
CORAL	93.31±3.73	61.11±1.66	70.62±0.87	70.95±0.36	74.00
+Tent	95.78±1.20	59.24±0.85	63.38±2.06	66.13±3.09	71.13
+TentBN	79.89±5.76	54.29±3.98	62.72±1.06	65.76±1.79	65.66
+TentClf	94.96±2.77	58.42±3.37	71.01±1.26	64.71±5.42	72.27
+SHOT	88.21±11.66	50.29±2.91	58.00±1.79	67.55±0.51	66.01
+SHOTIM	87.74±11.38	49.89±2.74	57.73±1.76	67.61±0.49	65.75
+PL	95.78±1.34	54.09±4.31	55.03±2.09	61.42±9.04	66.58
+PLClf	95.04±2.59	57.67±3.74	71.00±1.33	71.09±0.48	73.70
+T3A	97.10±3.42	63.61±3.43	67.90±0.78	73.34±1.26	75.49
+TAST (Ours)	95.36±7.76	62.95±3.23	69.06±1.05	71.89±1.95	74.82
+TAST-BN (Ours)	98.90±0.58	61.01±2.41	69.74±2.57	78.40±1.15	77.01

Table 19: Full results using classifiers trained by CORAL for Table 2 on PACS. We use ResNet-18 as a backbone network.

Method	A	C	P	S	Avg
CORAL	78.74±1.79	74.57±1.79	92.48±0.90	78.21±1.51	81.00
+Tent	82.11±0.95	81.22±1.02	95.15±0.04	78.20±1.33	84.17
+TentBN	80.06±0.86	77.14±1.35	94.05±0.31	77.87±0.50	82.28
+TentClf	77.14±0.99	63.00±6.22	92.93±1.12	69.77±2.86	75.71
+SHOT	82.92±1.33	81.13±1.18	95.28±0.60	79.37±1.05	84.67
+SHOTIM	82.92±1.24	81.06±1.17	95.30±0.57	79.23±1.10	84.63
+PL	83.44±1.79	67.36±9.25	94.20±2.49	60.82±12.65	76.46
+PLClf	79.72±1.06	62.98±8.19	93.12±0.60	68.81±1.23	76.16
+T3A	80.68±1.15	77.52±0.54	93.25±0.66	79.53±0.70	82.75
+TAST (Ours)	80.88±1.33	77.86±0.92	94.28±0.56	79.60±1.60	83.16
+TAST-BN (Ours)	86.96±0.66	83.58±1.32	96.59±0.62	81.69±1.16	87.21

Table 20: Full results using classifiers trained by CORAL for Table 2 on OfficeHome. We use ResNet-18 as a backbone network.

Method	A	C	P	R	Avg
CORAL	55.78±0.29	50.09±0.09	72.09±0.32	73.16±0.39	62.78
+Tent	55.33±0.33	50.79±0.31	71.08±0.32	72.29±0.41	62.37
+TentBN	56.59±0.34	51.54±0.07	72.19±0.19	73.17±0.30	63.37
+TentClf	55.56±0.40	49.96±0.16	72.07±0.44	73.00±0.44	62.65
+SHOT	55.77±0.29	52.67±0.44	72.22±0.64	73.50±0.28	63.54
+SHOTIM	55.72±0.28	52.64±0.39	72.23±0.63	73.52±0.29	63.53
+PL	54.17±1.83	46.74±4.73	71.53±0.40	72.34±0.89	61.19
+PLClf	55.77±0.38	50.04±0.44	71.90±0.37	73.03±0.42	62.68
+T3A	55.83±0.36	51.68±0.51	73.70±0.43	73.66±0.55	63.72
+TAST (Ours)	56.22±0.57	51.73±0.48	74.05±0.73	74.00±0.52	64.00
+TAST-BN (Ours)	54.71±0.40	52.07±0.61	72.80±0.65	72.33±0.49	62.98

Table 21: Full results using classifiers trained by CORAL for Table 2 on TerraIncognita. We use ResNet-18 as a backbone network.

Method	L100	L38	L43	L46	Avg
CORAL	38.41±2.79	25.98±6.65	45.59±2.53	36.08±1.75	36.51
+Tent	37.31±3.54	24.76±1.90	45.99±0.73	38.79±1.78	36.71
+TentBN	41.76±1.23	33.9±2.32	40.59±3.21	35.29±0.98	37.89
+TentClf	29.99±12.66	15.84±18.76	43.36±4.29	31.89±2.89	30.27
+SHOT	35.95±0.88	25.85±1.40	38.33±0.69	32.67±0.83	33.20
+SHOTIM	35.81±0.77	25.64±1.15	38.16±0.75	32.78±0.45	33.10
+PL	37.32±23.49	24.27±24.17	31.84±7.57	23.84±6.83	29.32
+PLClf	45.07±7.63	20.52±19.27	44.4±1.32	27.18±3.00	34.29
+T3A	37.14±2.17	34.49±3.47	45.00±3.91	36.91±1.86	38.39
+TAST (Ours)	46.01±2.18	32.11±4.30	43.31±3.17	35.42±2.53	39.21
+TAST-BN (Ours)	43.04±3.00	32.25±5.90	42.53±2.54	31.99±0.81	37.45

Table 22: Full results using classifiers trained by CORAL for Table 2 on VLCS. We use ResNet-50 as a backbone network.

Method	C	L	S	V	Avg
CORAL	96.82±1.06	62.51±0.81	71.46±1.71	74.79±3.23	76.39
+Tent	96.53±2.09	59.55±0.71	67.96±3.68	73.69±2.62	74.43
+TentBN	84.24±2.39	56.07±2.77	63.90±1.46	68.84±2.75	68.26
+TentClf	96.99±1.16	61.48±1.68	72.32±1.97	75.00±3.07	76.45
+SHOT	85.07±1.63	46.27±2.62	56.77±1.03	68.34±1.01	64.11
+SHOTIM	83.57±0.89	45.86±2.93	56.55±0.81	68.53±0.98	63.63
+PL	98.32±0.64	53.64±6.70	67.76±1.16	71.22±5.85	72.74
+PLClf	96.85±1.30	58.71±2.76	72.20±1.96	74.94±3.89	75.68
+T3A	98.24±0.70	64.69±1.64	73.06±2.04	73.34±3.81	77.33
+TAST (Ours)	99.15±0.28	64.17±2.37	72.32±1.75	73.27±3.27	77.23
+TAST-BN (Ours)	99.14±0.45	64.95±2.74	73.39±0.94	79.04±2.19	79.13

Table 23: Full results using classifiers trained by CORAL for Table 2 on PACS. We use ResNet-50 as a backbone network.

Method	A	C	P	S	Avg
CORAL	84.40±1.36	79.88±2.80	95.58±0.69	74.24±3.09	83.52
+Tent	86.12±1.37	85.15±1.85	96.28±0.78	78.47±1.52	86.50
+TentBN	84.34±0.98	81.63±2.47	96.38±0.50	77.86±1.10	85.05
+TentClf	84.68±1.88	80.32±2.89	95.98±1.01	67.59±8.18	82.14
+SHOT	85.75±1.92	82.38±2.52	96.88±0.92	75.37±2.56	85.09
+SHOTIM	85.72±1.82	82.38±2.43	96.84±0.94	75.29±1.96	85.06
+PL	84.87±3.66	77.93±3.78	96.29±0.73	44.74±20.19	75.96
+PLClf	85.43±1.52	79.81±3.15	96.21±0.91	72.78±5.06	83.56
+T3A	84.71±1.96	81.30±2.98	96.68±0.53	75.47±2.36	84.54
+TAST (Ours)	85.74±1.77	81.05±2.79	96.88±0.49	76.48±2.33	85.04
+TAST-BN (Ours)	90.95±1.20	86.78±1.39	98.17±0.43	85.72±0.63	90.41

Table 24: Full results using classifiers trained by CORAL for Table 2 on OfficeHome. We use ResNet-50 as a backbone network.

Method	A	C	P	R	Avg
CORAL	60.84±1.18	53.82±0.69	76.06±0.25	76.85±1.15	66.89
+Tent	61.11±1.05	54.16±0.56	73.61±0.66	76.31±1.28	66.30
+TentBN	61.91±1.17	55.73±0.67	76.28±0.47	76.82±1.09	67.68
+TentClf	54.31±1.96	49.96±1.28	75.30±0.08	76.56±1.64	64.03
+SHOT	61.79±1.61	56.93±0.72	75.97±0.79	76.23±1.08	67.73
+SHOTIM	61.75±1.52	56.93±0.79	75.94±0.81	76.24±0.95	67.72
+PL	54.78±3.96	40.71±10.95	74.19±0.49	73.28±1.81	60.74
+PLClf	59.80±0.85	53.40±1.46	75.60±0.17	76.15±1.39	66.24
+T3A	61.59±1.51	55.57±0.85	77.45±0.74	77.72±1.36	68.08
+TAST (Ours)	62.02±1.30	55.88±0.86	78.06±1.01	77.60±1.41	68.39
+TAST-BN (Ours)	63.45±1.48	59.01±1.14	76.68±0.74	77.00±1.13	69.04

Table 25: Full results using classifiers trained by CORAL for Table 2 on TerraIncognita. We use ResNet-50 as a backbone network.

Method	L100	L38	L43	L46	Avg
CORAL	45.52±0.53	39.33±2.81	48.98±2.28	37.35±2.71	42.79
+Tent	46.72±2.57	34.14±3.01	48.05±10.46	39.70±3.14	42.15
+TentBN	48.27±2.51	38.07±1.08	44.89±2.73	34.92±3.07	41.54
+TentClf	42.57±5.73	38.35±3.37	44.10±2.18	33.92±5.58	39.74
+SHOT	38.95±1.35	26.99±1.76	40.93±2.51	28.98±4.77	33.96
+SHOTIM	39.52±2.40	26.45±3.94	41.07±2.21	29.64±4.16	34.17
+PL	51.29±12.49	47.88±5.50	29.58±10.72	17.99±10.59	36.69
+PLClf	53.69±5.34	43.78±6.46	47.67±6.30	34.57±5.18	44.93
+T3A	45.57±1.04	40.31±1.50	49.81±2.10	38.31±1.60	43.50
+TAST (Ours)	53.81±0.58	39.99±2.38	48.07±3.86	35.02±3.12	44.22
+TAST-BN (Ours)	54.80±3.22	41.56±6.79	47.09±5.58	30.38±4.60	43.46

Table 26: Average accuracy(%) using classifiers trained by MMD for Table 2 of the main paper on the domain generalization benchmarks, namely VLCS, PACS, OfficeHome, and TerraIncognita. We use ResNet-18 as a backbone network.

Method	VLCS	PACS	OfficeHome	TerraIncognita	Avg
MMD	74.90±0.50	81.06±0.92	62.20±0.48	35.73±2.70	63.47
+Tent	74.59±0.66	84.47±0.19	62.15±0.33	36.11±0.72	64.33
+TentBN	65.94±1.91	82.44±0.26	62.80±0.46	37.66±0.34	62.21
+TentClf	74.91±0.60	57.76±5.32	62.10±0.50	28.94±6.56	55.93
+SHOT	65.41±2.03	85.57±0.28	63.25±0.53	32.34±0.68	61.64
+SHOTIM	65.00±2.20	85.53±0.29	63.20±0.56	32.25±0.55	61.50
+PL	66.17±1.73	74.42±4.09	60.49±1.03	22.30±8.42	55.85
+PLClf	74.84±0.50	69.95±0.95	62.16±0.45	31.94±5.67	59.72
+T3A	77.28±0.45	82.52±0.53	63.34±0.55	37.40±1.86	65.14
+TAST (Ours)	76.21±0.79	83.29±0.26	63.49±0.49	38.12±2.47	65.28
+TAST-BN (Ours)	76.06±0.89	86.35±0.76	63.22±0.26	39.46±1.63	66.27

Table 27: Full results using classifiers trained by MMD for Table 26 on VLCS. We use ResNet-18 as a backbone network.

Method	C	L	S	V	Avg
MMD	95.51±2.59	62.32±0.68	70.09±0.80	71.68±0.83	74.90
+Tent	97.20±0.55	61.53±0.60	69.32±2.58	70.33±0.92	74.59
+TentBN	80.71±5.21	54.94±2.31	61.88±0.30	66.25±1.58	65.94
+TentClf	95.71±2.16	61.87±1.02	70.15±0.91	71.90±0.82	74.91
+SHOT	88.10±8.59	48.99±2.74	57.14±1.13	67.43±0.47	65.41
+SHOTIM	86.93±8.90	48.71±2.70	56.98±1.17	67.37±0.48	65.00
+PL	95.63±1.07	51.75±2.10	59.89±11.04	57.40±6.85	66.17
+PLClf	95.69±2.19	61.65±0.85	70.14±0.86	71.87±0.79	74.84
+T3A	99.15±0.52	64.19±0.76	71.16±0.74	74.62±1.63	77.28
+TAST (Ours)	99.29±0.46	63.14±0.66	69.62±1.23	72.81±1.30	76.21
+TAST-BN (Ours)	99.14±0.48	61.54±2.74	65.03±1.95	78.53±0.35	76.06

Table 28: Full results using classifiers trained by MMD for Table 26 on PACS. We use ResNet-18 as a backbone network.

Method	A	C	P	S	Avg
MMD	79.52±0.50	74.66±1.28	93.46±0.95	76.60±2.62	81.06
+Tent	82.84±0.97	81.22±0.85	95.49±0.40	78.32±0.48	84.47
+TentBN	80.51±0.84	77.09±0.44	94.55±0.33	77.59±0.64	82.44
+TentClf	56.53±16.38	47.89±6.86	93.37±0.67	33.26±8.17	57.76
+SHOT	84.50±0.13	81.98±0.98	95.58±0.22	80.19±0.95	85.57
+SHOTIM	84.49±0.20	81.94±0.93	95.58±0.22	80.09±0.89	85.53
+PL	84.59±0.48	53.96±10.45	95.10±0.18	64.04±11.28	74.42
+PLClf	80.04±0.60	63.87±8.49	93.60±0.57	42.28±7.47	69.95
+T3A	81.92±0.41	75.35±1.11	94.99±0.36	77.81±1.62	82.52
+TAST (Ours)	81.76±0.31	77.13±0.51	95.37±0.70	78.91±1.12	83.29
+TAST-BN (Ours)	86.23±1.18	82.16±1.93	97.46±0.14	79.55±1.08	86.35

Table 29: Full results using classifiers trained by MMD for Table 26 on OfficeHome. We use ResNet-18 as a backbone network.

Method	A	C	P	R	Avg
MMD	54.39±0.86	49.71±1.02	71.95±0.59	72.74±0.41	62.20
+Tent	55.73±0.47	49.71±0.20	70.75±0.74	72.41±0.45	62.15
+TentBN	55.34±0.56	51.09±1.09	72.11±0.46	72.68±0.27	62.80
+TentClf	54.39±0.72	49.28±1.18	71.95±0.66	72.77±0.27	62.10
+SHOT	54.83±0.77	52.38±0.95	72.59±0.71	73.18±0.15	63.25
+SHOTIM	54.85±0.85	52.27±0.97	72.54±0.71	73.15±0.17	63.20
+PL	53.26±1.14	44.63±3.44	71.76±0.68	72.33±0.08	60.49
+PLClf	54.44±0.67	49.67±0.97	71.97±0.65	72.57±0.29	62.16
+T3A	54.43±1.26	51.25±0.83	73.86±0.57	73.84±0.47	63.34
+TAST (Ours)	55.17±1.04	50.80±1.14	74.20±0.57	73.78±0.51	63.49
+TAST-BN (Ours)	54.40±0.60	52.21±0.38	73.30±0.35	72.96±0.42	63.22

Table 30: Full results using classifiers trained by MMD for Table 26 on TerraIncognita. We use ResNet-18 as a backbone network.

Method	L100	L38	L43	L46	Avg
MMD	34.57±3.77	26.57±6.18	46.08±2.85	35.72±1.17	35.73
+Tent	37.04±3.72	25.40±1.81	44.82±0.72	37.19±1.64	36.11
+TentBN	40.04±2.45	33.38±2.98	42.38±2.80	34.84±1.06	37.66
+TentClf	22.92±9.25	15.19±15.33	45.24±4.15	32.39±1.27	28.94
+SHOT	33.79±1.34	25.68±2.73	37.81±0.67	32.07±2.71	32.34
+SHOTIM	33.48±1.14	25.77±1.95	37.87±0.61	31.87±2.44	32.25
+PL	29.45±26.19	13.78±20.60	27.69±10.39	18.27±5.75	22.30
+PLClf	36.96±8.00	17.63±18.15	46.28±4.42	26.87±2.41	31.94
+T3A	35.16±2.74	34.41±2.73	43.83±4.22	36.19±1.79	37.40
+TAST (Ours)	44.70±1.82	31.97±4.96	42.30±4.83	33.50±4.40	38.12
+TAST-BN (Ours)	43.81±5.05	37.35±2.57	44.41±1.55	32.28±1.73	39.46

Table 31: Average accuracy(%) using classifiers trained by Mixup for Table 2 of the main paper on the domain generalization benchmarks, namely VLCS, PACS, OfficeHome, and TerraIncognita. We use ResNet-18 as a backbone network.

Method	VLCS	PACS	OfficeHome	TerraIncognita	Avg
Mixup	74.97±0.86	78.29±0.88	61.83±0.88	41.04±1.01	64.03
+Tent	72.73±0.41	83.88±0.51	61.82±0.45	39.52±0.36	64.49
+TentBN	62.83±0.83	81.44±0.27	62.82±0.64	40.72±1.81	61.95
+TentClf	74.33±0.92	68.95±2.86	61.45±0.88	37.21±4.79	60.49
+SHOT	68.69±0.91	84.43±0.39	62.81±0.42	36.32±0.50	63.06
+SHOTIM	68.31±0.98	84.52±0.36	62.80±0.43	36.03±0.61	62.92
+PL	59.90±2.19	68.02±2.43	60.66±0.63	32.30±6.83	55.22
+PLClf	74.19±0.78	70.94±3.00	61.67±0.86	40.63±4.88	61.86
+T3A	78.43±0.76	81.91±0.54	63.49±0.86	39.89±0.90	65.93
+TAST (Ours)	77.19±0.80	82.85±0.36	63.83±0.74	41.44±1.67	66.33
+TAST-BN (Ours)	76.89±0.86	87.14±0.56	62.09±0.86	42.70±1.90	67.21

Table 32: Full results using classifiers trained by Mixup for Table 31 on VLCS. We use ResNet-18 as a backbone network.

Method	C	L	S	V	Avg
Mixup	94.73±1.35	62.52±0.79	69.70±0.89	72.93±1.27	74.97
+Tent	95.27±0.47	59.84±1.01	68.61±1.04	67.19±1.62	72.73
+TentBN	76.52±1.36	52.40±1.05	60.00±1.63	62.41±2.25	62.83
+TentClf	94.87±1.31	61.72±0.73	68.44±1.04	72.29±2.22	74.33
+SHOT	96.47±3.75	51.01±1.22	58.83±1.55	68.47±0.27	68.69
+SHOTIM	95.63±4.31	50.49±1.13	58.71±1.71	68.41±0.35	68.31
+PL	94.94±1.82	49.88±0.35	45.87±7.30	48.90±4.44	59.90
+PLClf	94.82±1.29	59.16±0.65	69.85±0.94	72.92±1.54	74.19
+T3A	99.11±0.76	64.75±1.02	72.69±2.16	77.16±0.79	78.43
+TAST (Ours)	98.97±0.87	63.19±0.77	71.04±1.80	75.56±1.03	77.19
+TAST-BN (Ours)	99.27±0.32	60.76±4.75	69.63±2.58	77.91±1.76	76.89

Table 33: Full results using classifiers trained by Mixup for Table 31 on PACS. We use ResNet-18 as a backbone network.

Method	A	C	P	S	Avg
Mixup	80.28±2.31	70.69±1.19	94.26±0.85	67.94±0.73	78.29
+Tent	81.51±0.82	79.49±1.01	95.58±0.18	78.94±1.04	83.88
+TentBN	82.40±1.00	75.98±0.79	94.63±0.45	72.75±1.57	81.44
+TentClf	79.66±3.73	64.24±4.07	94.17±1.01	37.75±13.33	68.95
+SHOT	85.20±0.56	80.13±0.88	96.20±0.75	76.18±0.45	84.43
+SHOTIM	85.17±0.56	80.64±0.92	96.22±0.77	76.05±0.50	84.52
+PL	82.82±2.54	66.48±8.08	95.40±0.64	27.37±5.71	68.02
+PLClf	79.32±2.88	70.61±1.26	94.26±0.89	39.58±15.47	70.94
+T3A	83.06±1.31	75.92±0.58	95.87±0.66	72.80±2.09	81.91
+TAST (Ours)	83.93±0.99	76.75±1.32	96.34±0.63	74.39±1.69	82.85
+TAST-BN (Ours)	86.18±0.49	82.69±1.44	97.27±0.48	82.43±1.80	87.14

Table 34: Full results using classifiers trained by Mixup for Table 31 on OfficeHome. We use ResNet-18 as a backbone network.

Method	A	C	P	R	Avg
Mixup	53.92±1.21	49.17±1.49	71.66±0.52	72.56±0.82	61.83
+Tent	53.22±0.92	50.75±0.79	71.22±0.74	72.10±0.62	61.82
+TentBN	54.78±1.29	51.47±1.09	72.21±0.25	72.82±0.74	62.82
+TentClf	53.87±1.20	48.22±1.48	71.65±0.42	72.06±0.84	61.45
+SHOT	53.95±1.17	52.20±1.27	72.29±0.36	72.79±0.43	62.81
+SHOTIM	53.94±1.22	52.15±1.30	72.28±0.42	72.83±0.41	62.80
+PL	52.82±0.96	48.17±1.38	70.97±0.82	70.70±1.00	60.66
+PLClf	53.85±1.10	49.12±1.43	71.64±0.47	72.06±1.04	61.67
+T3A	54.83±1.49	50.97±1.51	74.14±0.63	74.00±0.31	63.49
+TAST (Ours)	54.97±0.96	51.31±1.84	74.88±0.66	74.16±0.22	63.83
+TAST-BN (Ours)	53.09±1.44	51.04±1.81	72.44±0.64	71.80±0.64	62.09

Table 35: Full results using classifiers trained by Mixup for Table 31 on TerraIncognita. We use ResNet-18 as a backbone network.

Method	L100	L38	L43	L46	Avg
Mixup	52.26±1.44	35.90±4.46	41.23±2.04	34.77±2.14	41.04
+Tent	41.35±2.74	33.05±2.75	44.17±1.50	39.51±1.83	39.52
+TentBN	45.35±2.22	44.17±2.15	42.25±1.98	31.11±2.43	40.72
+TentClf	49.62±7.17	37.29±12.05	37.45±2.99	24.48±0.73	37.21
+SHOT	42.78±3.48	31.04±2.88	39.58±1.29	31.86±3.47	36.32
+SHOTIM	42.14±3.38	30.71±3.18	39.37±1.34	31.89±3.51	36.03
+PL	52.56±0.16	34.80±21.65	23.33±4.85	18.51±6.10	32.30
+PLClf	53.30±1.59	35.52±18.76	40.68±1.15	33.04±2.57	40.63
+T3A	43.05±2.28	38.53±2.37	43.32±3.33	34.65±1.22	39.89
+TAST (Ours)	57.57±5.18	36.43±3.72	38.34±2.38	33.40±2.08	41.44
+TAST-BN (Ours)	56.81±4.34	42.44±2.03	41.01±2.50	30.54±1.52	42.70

Table 36: Full results using classifiers trained by ERM for Table 3 on VLCS. We use ResNet-18 as a backbone network.

Method	N_e	C	L	S	V	Avg
ERM	-	94.70±1.33	63.79±1.30	67.90±1.97	73.15±1.37	74.88
+T3A	-	97.52±1.99	65.32±2.24	70.70±3.48	75.51±1.75	77.26
+TAST-N (Ours)	-	95.31±4.33	65.62±1.79	68.9±3.22	74.96±1.66	76.20
+TAST (Ours)	1	98.62±1.06	62.61±1.90	66.84±3.01	72.73±1.17	75.20
+TAST (Ours)	5	99.15±0.68	65.58±3.08	67.53±1.49	74.46±1.87	76.68
+TAST (Ours)	10	99.22±0.45	66.21±1.36	68.62±2.39	75.66±2.03	77.43
+TAST (Ours)	20	99.17±0.60	65.87±1.90	68.13±1.76	75.92±1.75	77.27

Table 37: Full results using classifiers trained by ERM for Table 3 on PACS. We use ResNet-18 as a backbone network.

Method	N_e	A	C	P	S	Avg
ERM	-	77.78±0.81	75.09±1.22	95.19±0.29	69.11±1.22	79.29
+T3A	-	78.81±0.97	77.14±1.20	95.92±0.36	71.44±1.63	80.83
+TAST-N (Ours)	-	80.18±0.88	77.34±1.38	96.57±0.27	72.38±0.77	81.62
+TAST (Ours)	1	80.21±0.80	77.06±1.44	96.13±0.53	71.51±1.22	81.23
+TAST (Ours)	5	80.85±0.86	77.91±0.71	96.49±0.37	72.00±1.16	81.81
+TAST (Ours)	10	79.95±1.42	78.12±0.98	96.51±0.25	71.65±2.32	81.56
+TAST (Ours)	20	80.56±0.53	78.26±0.99	96.44±0.20	72.52±0.77	81.94

Table 38: Full results using classifiers trained by ERM for Table 3 on OfficeHome. We use ResNet-18 as a backbone network.

Method	N_e	A	C	P	R	Avg
ERM	-	55.19±0.49	47.76±1.02	72.22±0.53	73.21±0.89	62.10
+T3A	-	55.10±0.74	49.56±1.14	74.10±0.55	74.07±1.18	63.21
+TAST-N (Ours)	-	55.25±0.97	50.45±1.03	74.24±0.55	74.23±1.37	63.54
+TAST (Ours)	1	53.53±0.90	49.46±1.39	72.84±0.69	72.53±1.30	62.09
+TAST (Ours)	5	55.34±1.04	50.51±1.03	74.23±0.43	73.97±0.95	63.51
+TAST (Ours)	10	55.76±0.68	49.52±1.38	74.17±0.49	74.11±1.00	63.39
+TAST (Ours)	20	56.15±0.68	50.04±1.31	74.33±0.28	74.28±1.23	63.70

Table 39: Full results using classifiers trained by ERM for Table 3 on TerraIncognita. We use ResNet-18 as a backbone network.

Method	N_e	L100	L38	L43	L46	Avg
ERM	-	37.18±2.46	36.12±4.20	53.18±1.27	36.02±1.37	40.62
+T3A	-	36.22±1.89	40.08±1.98	50.72±1.02	33.79±1.25	40.20
+TAST-N (Ours)	-	39.75±1.76	39.20±2.65	52.33±2.63	36.24±1.28	41.88
+TAST (Ours)	1	43.23±0.87	42.49±2.08	51.22±3.69	33.41±1.05	42.59
+TAST (Ours)	5	43.95±2.33	38.89±2.42	52.44±3.04	35.42±1.27	42.68
+TAST (Ours)	10	43.96±2.92	38.48±3.56	53.27±2.73	34.67±1.24	42.60
+TAST (Ours)	20	43.67±2.83	39.24±3.79	52.64±3.02	35.01±1.09	42.64

Table 40: Full results for Table 4 in the online setting on CIFAR-10C with seed 0.

Method	gauss	brit	contr	defoc	elast	fog	frost	glass	impul	jpeg	motn	pixel	shot	snow	zoom
SHOT	17.33	8.57	8.66	9.70	19.56	19.85	13.82	25.59	27.28	13.99	14.20	11.67	15.99	15.89	8.10
Tent	16.01	7.78	7.93	9.39	18.26	16.07	12.53	23.32	24.65	13.26	12.53	10.99	14.74	13.82	7.86
PL	33.74	7.52	11.60	10.52	20.16	23.95	21.77	38.39	43.84	16.89	18.82	29.60	30.48	18.63	9.53
T3A	41.55	7.92	13.63	13.75	22.35	28.66	27.78	45.90	55.44	19.15	23.43	41.19	40.14	22.11	11.23
TAST (Ours)	41.90	7.34	13.56	11.71	21.33	28.70	26.37	45.05	54.79	19.07	22.76	36.82	37.55	21.79	10.70
TAST-BN (Ours)	14.97	7.77	7.86	8.58	16.50	15.24	12.20	21.88	23.11	12.34	11.66	10.29	13.91	12.86	7.86
TTT++	16.16	7.30	7.43	9.04	18.13	17.77	12.40	25.76	26.65	13.01	12.82	11.28	15.11	14.35	7.57

Table 41: Full results for Table 4 in the online setting on CIFAR-10C with seed 1.

Method	gauss	brit	contr	defoc	elast	fog	frost	glass	impul	jpeg	motn	pixel	shot	snow	zoom
SHOT	17.09	8.67	8.61	9.86	19.58	19.79	13.78	25.37	27.11	14.15	13.98	11.80	16.12	15.81	8.22
Tent	15.97	8.03	8.01	8.97	17.93	16.53	12.68	23.47	24.84	13.18	12.77	11.04	14.21	13.87	7.72
PL	33.43	7.57	11.54	10.64	20.36	23.87	21.85	38.45	43.70	16.89	18.92	29.86	30.37	18.80	9.32
T3A	42.32	7.67	13.68	12.84	22.39	28.96	27.88	46.15	55.76	19.31	23.24	41.15	40.22	22.21	11.26
TAST (Ours)	41.79	7.48	13.52	11.92	21.38	28.42	26.54	45.13	53.78	18.82	22.42	36.96	37.76	22.11	10.62
TAST-BN (Ours)	14.85	7.50	8.01	8.64	17.15	15.06	12.19	21.86	22.44	12.46	12.02	10.56	13.58	12.81	7.34
TTT++	16.36	7.20	7.40	9.09	18.28	17.73	12.38	25.85	26.45	13.13	12.80	11.39	15.00	14.38	7.64

Table 42: Full results for Table 4 in the online setting on CIFAR-10C with seed 2.

Method	gauss	brit	contr	defoc	elast	fog	frost	glass	impul	jpeg	motn	pixel	shot	snow	zoom
SHOT	17.15	8.56	8.54	9.85	19.57	19.41	14.10	25.68	26.90	13.98	14.02	11.45	15.99	16.11	8.37
Tent	16.08	7.88	7.93	9.56	18.35	17.19	12.86	23.42	24.13	13.28	12.96	10.91	14.51	14.53	7.68
PL	33.72	7.59	11.57	10.65	20.30	23.92	21.93	38.08	43.83	16.95	18.65	29.95	30.69	18.93	9.47
T3A	41.54	7.96	13.70	12.82	22.34	28.86	28.17	46.39	55.48	19.26	23.40	41.29	40.29	22.30	11.29
TAST (Ours)	42.49	7.26	13.54	11.91	21.50	28.41	26.88	45.03	54.26	19.06	22.50	37.44	37.61	21.94	10.72
TAST-BN (Ours)	14.89	7.82	7.81	8.54	16.97	15.51	12.61	21.63	22.55	12.32	11.65	10.37	13.79	13.14	7.57
TTT++	16.39	7.28	7.52	9.16	18.12	17.63	12.37	25.81	26.40	13.16	12.86	11.47	15.06	14.44	7.42

Table 43: Full results for Table 4 in the online setting on CIFAR-10C with seed 3.

Method	gauss	brit	contr	defoc	elast	fog	frost	glass	impul	jpeg	motn	pixel	shot	snow	zoom
SHOT	16.78	8.76	8.47	9.91	19.41	19.83	14.03	25.74	27.30	13.78	13.84	11.80	15.97	15.74	8.19
Tent	15.56	7.95	7.52	9.14	17.97	16.01	12.40	23.69	24.46	13.04	12.53	10.79	14.90	14.00	7.45
PL	33.33	7.49	11.41	10.59	20.01	23.71	21.56	38.51	43.20	16.79	18.48	29.90	30.18	18.63	9.38
T3A	42.08	8.12	13.75	12.97	22.28	28.83	27.77	46.22	55.53	19.17	23.29	41.17	40.49	22.32	11.32
TAST (Ours)	41.89	7.28	13.58	11.92	21.31	28.78	26.23	44.73	53.93	18.90	22.54	37.08	37.57	21.52	10.54
TAST-BN (Ours)	14.94	7.62	7.55	8.71	16.60	14.61	12.00	21.89	22.06	12.41	11.35	10.15	13.78	13.16	7.49
TTT++	16.11	7.29	7.47	9.16	18.14	17.74	12.31	25.53	26.20	13.22	12.93	11.39	14.88	14.41	7.71